

LINKÖPING UNIVERSITY MEDICAL DISSERTATIONS NO 1450

# Guided Regeneration of the Human Skin

## - *in vitro* and *in vivo* studies

Erika Nyman



**Linköping University**  
**FACULTY OF HEALTH SCIENCES**

Division of Clinical Sciences  
Department of Clinical and Experimental Medicine  
Faculty of Health Sciences, Linköping University  
SE-851 85 Linköping, Sweden

2015

© Erika Nyman

Printed in Sweden by LiU-tryck, Linköping, Sweden, 2015

Permission to print the published articles (Papers I, II, and III) is granted from the copyright holders.

ISBN: 978-91-7519-114-0

ISSN: 0345-0082

*"Jag förstår att mamma håller på med något viktigt men är det inte bara att sätta på ett plåster?"*

Elvin åtta år

*To Tobbe, Elvin, Anton and Mira*

**SUPERVISOR**

Gunnar Kratz, PhD, Professor  
Department of Clinical and Experimental Medicine  
Linköping University

**CO-SUPERVISORS**

Fredrik Huss, PhD, Associate Professor  
Department of Surgical Sciences, Plastic Surgery  
Uppsala University

Joakim Henricson, PhD  
Department of Clinical and Experimental Medicine  
Linköping University

# Table of Contents

Abstract .....	7
Selected Abbreviations .....	9
List of Original Papers .....	11
Introduction.....	13
Wound healing.....	13
Scaffolds, Tissue engineering, and Guided tissue regeneration of the skin.....	21
The fetal environment .....	23
Hyaluronic acid.....	23
Wound models and Wound-healing measurements.....	24
Cell culture .....	24
Three-dimensional <i>in vitro</i> models.....	25
The skin blister model.....	25
Skin biopsy models .....	25
Visual inspection and imaging.....	25
Surface area measurements.....	26
Animal models.....	26
Wound models used in this thesis .....	26
Aims of the Thesis .....	29
Material and Methods.....	31
Cell culture (Paper I) .....	31
Scaffold materials (Papers I and II) .....	32
Poly(urethane urea) (Paper I) .....	32
Macroporous gelatin spheres (Paper II).....	34
Culture conditions (Papers I and III) .....	35
Culture media (Papers I and III).....	35

Fibroblast culture medium (Paper I).....	35
Wound culture media (Paper III).....	36
Collection of human amniotic fluid .....	36
<i>In vitro</i> wounds and Wound culture (Paper III).....	37
Routine histology (Papers I-IV) .....	38
Immunohistochemistry (Papers I and II) .....	39
Subjects (Papers I, II, and IV) .....	39
Paper I .....	39
Paper II.....	41
Paper IV .....	43
Tissue viability imaging (Paper IV) .....	45
Proteomics (Paper IV) .....	47
Statistics.....	48
Ethical approvals and Ethical considerations.....	49
Main Results and Discussion.....	53
Paper I.....	53
Paper II .....	58
Paper III.....	61
Paper IV.....	64
Concluding Remarks and Future Perspectives.....	75
Popular Scientific Summary in Swedish.....	79
Acknowledgements.....	83
References .....	87

# Abstract

Every day and in all parts of the world, humans experience different grades of wounding and tissue loss of the skin, thus initiating one of the most complex biological processes. Acute and chronic wounds, as well as the additional problem of skin scarring, involve not only great suffering for the patient but also extensive health care costs for the society. Although the wound-healing process is a well-studied field much knowledge must be gained to unlock the door to regenerative pathways in humans.

Epidermis heals by complete regeneration, but dermal and full thickness injuries heal with fibrosis and scar formation. In Papers I and II, we studied whether dermal scarring could be turned into regeneration by using two different types of three-dimensional dermal scaffolds. In Paper I, we studied a solid scaffold made of poly(urethane urea), initially *in vitro* then followed by *in vivo* studies. In Paper II, we intradermally injected a liquid three-dimensional scaffold consisting of porous gelatin spheres in human healthy volunteers. Both materials showed ingrowth of functional fibroblasts and blood vessels and appeared to stimulate regeneration while slowly degrading. This finding could be of significant clinical importance, for example in burn wound care or after cancer surgery.

In Papers III and IV, we wanted to study the effects of amniotic fluid and hyaluronic acid on adult wound healing, because early fetal wounds re-epithelialize rapidly and naturally heal dermis by regeneration without the need of a dermal scaffold. Amniotic fluid, naturally rich in hyaluronic acid, induced an accelerated re-epithelialization of adult human wounds *in vitro*, and hyaluronic acid seemed to be important for this effect. Stimulation with exogenous hyaluronic acid *in vivo* induced accelerated re-epithelialization and an altered protein expression in healthy human volunteers. The inflammatory phase of wound healing, as measured by tissue viability imaging, was not affected by hyaluronic acid. Elucidating the effects of amniotic fluid and hyaluronic acid on the wound-healing process may allow improved treatment of wounds with impaired healing.

Studies on finding new dermal scaffolds and studies on the positive effect of amniotic fluid or hyaluronic acid on the wound-healing process are two different ways of gaining insight that may lead to regeneration and improved wound healing for the patient.



# Selected Abbreviations

2-DE	Two-dimensional gel electrophoresis
AF	Amniotic fluid
ECM	Extracellular matrix
DMEM	Dulbecco's Modified Eagle's Medium
FCS	Fetal calf serum
HA	Hyaluronic acid
NCS	Newborn calf serum
PBS	Phosphate buffered saline
PUUR	Poly(urethane urea)
ROI	Region of interest
TE	Tissue engineering
TiVi	Tissue viability imaging



# List of Original Papers

This thesis is based upon the following papers, which will be referred to in the text by their roman numerals:

- I** Fredrik Huss, **Erika Nyman**, Carl-Johan Gustafson, Katrin Gissselfält, Elisabeth Liljensten, and Gunnar Kratz  
*Characterization of a new degradable polymer scaffold for regeneration of the dermis: In vitro and in vivo human studies*  
Organogenesis, 2008. 4(3): p. 195-200
- II** Fredrik Huss, **Erika Nyman**, Johanna Bolin, and Gunnar Kratz  
*Use of macroporous gelatine spheres as a biodegradable scaffold for guided tissue regeneration of healthy dermis in humans: an in vivo study*  
J Plast Reconstr Aesthet Surg, 2010. 63(5): p. 848-57
- III** **Erika Nyman**, Fredrik Huss, Torbjörn Nyman, and Gunnar Kratz  
*Hyaluronic acid, an important factor in the wound healing properties of amniotic fluid: in vitro studies of re-epithelialisation in human skin wounds.*  
J Plast Surg Hand Surg, 2013. 47(2): p. 89-92.
- IV** **Erika Nyman**, Joakim Henricson, Jonathan Rakar, Patrik Olausson, Bijar Ghafouri, Chris Anderson, and Gunnar Kratz  
*Exogenous hyaluronic acid induces accelerated re-epithelialization and altered protein expression in adult human skin wounds in vivo*  
Manuscript



# Introduction

Every day and in all parts of the world, humans experience different grades of wounding and tissue loss of the skin, thus initiating one of the most complex biological processes. The skin is the physical barrier between the organism and the environment, and its ability to heal is essential to survival. The skin has an impressive capacity to register and tolerate different stimuli, but physical, thermal, and chemical provocation can all cause injury when exceeding a certain level. Wound healing is a sophisticated, dynamic, and carefully regulated process that involves inflammation, new tissue formation, and remodeling. The elusive process of wound healing has been extensively studied but still leaves questions yet to be answered.

Acute and chronic wounds, as well as the additional problem with skin scarring, mean not only great suffering for the patient but also extensive health care costs for society [1].

## Wound healing

Wound healing aims at barrier restoration. A wound can be of different size and depth. A child falls and scratches her knee. As a result, the epidermis, the outermost layer, is disrupted (Figure 1). Keratinocytes release pre-stored interleukin-1 (IL-1), which notifies surrounding cells about the injury [2]. Mitotically active epidermal

cells, found in the *stratum basale*, break their contact inhibition, enlarge, divide, and migrate across the wound until it is re-epithelialized [3]. Epidermis is healed by complete regeneration and, no scar is formed (Figure 3).

If the wound reaches into the dermal tissue (Figure 2), it will cause bleeding from damaged vessels. Blood components are released, and a blood clotting cascade starts, resulting in the formation of a blood clot and hemostasis. Degranulation of platelets releases factors such as epidermal growth factor (EGF), platelet-derived growth factor (PDGF), and transforming growth factor- $\beta$  (TGF- $\beta$ ), as well as IL-1. As a part of the inflammatory process, PDGF and IL-1 are important in recruiting neutrophils. Monocytes are converted to macrophages, also central in inflammation as well as in tissue debridement. The inflammatory cells initiate the development of granulation tissue and release pro-inflammatory cytokines and growth factors [4]. Subsequently, keratinocytes are activated by expression of cytokines and growth factors [3] and move forward by crawling using lamellipodia [5].

Re-epithelialization, which is defined as the covering of the bared dermal surface, is a crucial parameter of successful wound healing [5]. The capacity of the epidermis to regenerate depends on populations of epidermal stem cells located in the hair follicles, sebaceous glands, and *stratum basale* [6, 7]. Ductal progenitors of the sweat gland have similarities to the hair follicle stem cells and have been shown to regenerate glabrous epidermis surrounding the sweat gland opening [8]. The undifferentiated keratinocytes ascend and mature through the layers of the epidermis while transforming into a cornified epithelium.

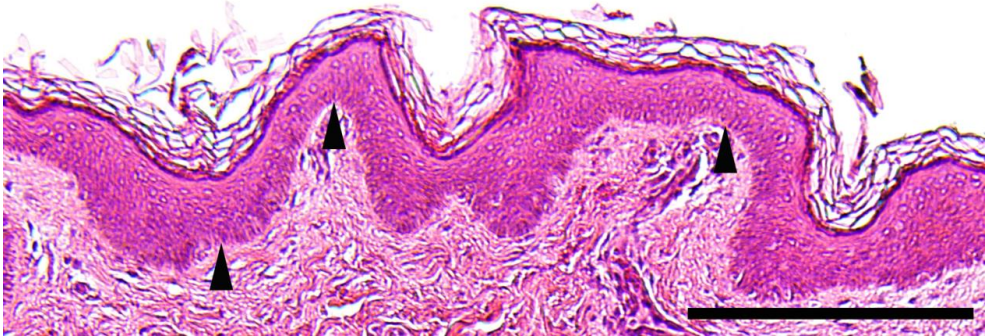


**Figure 1.** Structure of the epidermis. Histological picture of normal epidermis stained with hematoxylin and eosin. The epidermis is composed mainly of keratinocytes, but also includes for example melanocytes, Langerhans cells, and Merkel cells. In unwounded skin, new keratinocytes are produced in the *stratum basale* by cell division and are pushed to the surface while producing keratin, to gradually keratinize. The cytoplasm and nucleus disappear, and the cells flatten and eventually die, shed, and are replaced by new cells. The undifferentiated keratinocytes in the *stratum basale* change into cornified and non-dividing cells while they ascend through the *stratum spinosum*, the *stratum granulosum*, and finally the *stratum corneum* [9]. Arrowheads indicate stratum basale (bar = 250  $\mu\text{m}$ ).

As a response to dermal injury, resident dermal fibroblasts begin to proliferate. Three to four days after wounding, they migrate into the provisional matrix formed by fibrin threads during earlier coagulation [10]. The fibroblast activation is a rate limiting step of granulation tissue formation [11]. About a week after wounding, the blood clot is invaded by activated fibroblasts that synthesize collagen and glycoproteins to form a collagen rich matrix [12]. A proportion of the fibroblasts transform into specialized myofibroblasts in the granulation tissue. They contract the wound and help in wound closing [11, 13]. During the proliferative phase, the fibroblasts continue to deposit collagen, mainly type III, in random patterns [14].

Macrophages and damaged endothelial cells release factors for activation of endothelial cells. The endothelial cells proliferate to invade the neo-dermis. The

wound connective tissue is now pink and called granulation tissue because of the granular appearance of the numerous capillaries [11]. The granulation tissue is essential to the organization of a new extracellular matrix (ECM). Endothelial cells can also be recruited from bone-marrow-derived endothelial progenitor cells, but the magnitude of this contribution is thought to be small [15].

The final phase of wound repair involves remodeling, maturation, and scar formation. The scab is sloughed off, epidermis thickened, and blood vessels restored. This phase usually begins two to three weeks after wounding and can last for a year or more. Almost all endothelial cells, macrophages and myofibroblasts undergo apoptosis or exit the wound. Over six to twelve months the acellular ECM is actively remodeled, and the collagen fibers become more organized [16]. In the intermediate phases, the collagen fibers become tightly packed and are stabilized by formation of inter- and intramolecular crosslinks [17]. Collagen type III is remodeled to collagen type I by mainly matrix metalloproteinases that are secreted by fibroblasts, macrophages, and endothelial cells [16, 18, 19].



A young man is trapped in a burning shed. The fire rescue team manages to get him out of the fire, but he is severely injured, with deep dermal and full-thickness burn wounds. Initially, managing the airway, supporting ventilation, and initiating fluid resuscitation are absolutely crucial to survival [20], but after a major burn injury, the wound itself will also generate local and systemic symptoms. It is absolutely necessary to debride the wounded tissue [21].

If the epidermis and superficial dermis are wounded, the surface can heal through regeneration of the epidermis from adnexal organs (hair follicles, sebaceous- and sweat glands). When injury involves deeper parts of the dermis, the repair process is even more complex, and the wound heals with scar formation. In a deep dermal or full-thickness wound, there are no adnexal structures to regenerate the epidermis from, and there is little or no dermal tissue.

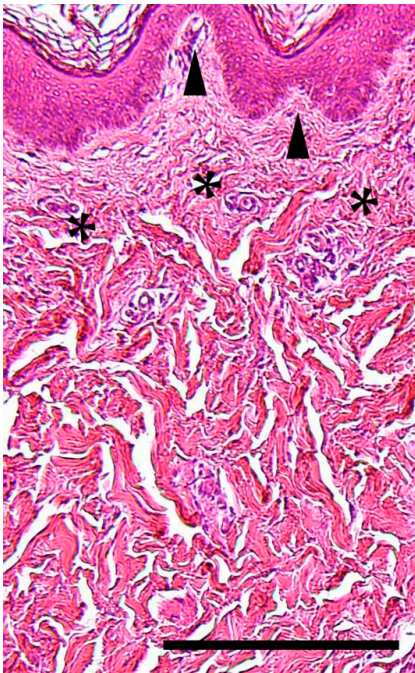


**Figure 2.** The dermis varies in thickness depending on the location of the body and confers strength and pliability to the skin. It consists mainly of fibroblasts and the extracellular matrix, but also macrophages, capillaries, lymphatic vessels, nerve endings, hair follicles, sweat glands, and sebaceous glands. The two diffusely delimited layers of the dermis are the *stratum papillare*, a thin outer layer with projections into the epidermis, and the *stratum reticulare*, a thick layer of dense irregular connective tissue. Collagen, mainly types I and III, is synthesized by the fibroblasts and forms the extracellular matrix together with elastic fibers, proteoglycans, and glycosaminoglycans. Arrowheads indicate the projections of *stratum papillare* into the epidermis and asterisks mark the transition zone from *stratum reticulare* to *stratum papillare* (bar = 250  $\mu$ m) [22, 23].

The conventional approach to treating deep burns is to apply autologous split-thickness skin grafts. Surgeons harvest and transplant healthy epidermis and a

variable amount of dermis to the injured and debrided area. The grafts provides a complete epidermal component for the wound, but is often insufficient as a dermal substitute [24]. Since the early 1980s, physicians have used cultured autologous keratinocytes to treat serious burns [25]. An unlimited amount of epidermis can be obtained, but the dermis is still completely left to heal by scarring.

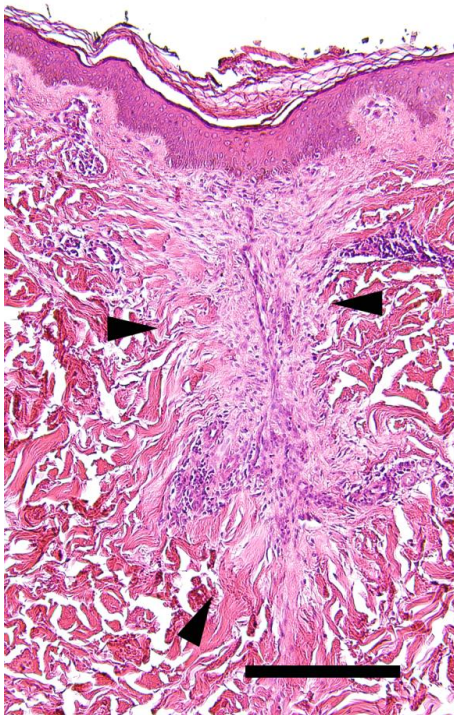


**Figure 3.** A deep dermal incisional wound after 14 days of healing. Epidermis is completely healed by regeneration while dermis is healed by scar formation. Arrowheads indicate dermal scar formation (bar = 250  $\mu\text{m}$ ).



At the nursing home, an elderly lady is cared for by the nurse's assistant. She needs frequent changes of wound dressings and repeated surgical debridement of her ischemic leg ulcer. Chronic wounds affect primarily elderly or disabled persons [26],

and are often caused by edema and poor circulation [27]. Typical characteristics of a chronic wound are accumulation of devitalized tissue, hyperkeratotic tissue, infection, decreased angiogenesis, and increased proteases [28]. Debridement aims to remove devitalized tissue, decrease bacterial contamination, and stimulate contraction and epithelialization. Biopsies from non-healing wound edges exhibit a distinct pathogenic morphology, with a hyperkeratotic epidermis and dermal fibrosis with increased pro-collagen production. The fibroblasts exhibit impaired migratory capacity. A recent study has hypothesized that the chronic ulcer contains subpopulations of cells with different capacity to heal and different gene expression profiles as compared to cells from adjacent non-ulcerated biopsies [29].



In another part of the world, a couple is going to the gynecologist to have an amniocentesis done in week 15 of pregnancy. The biopsy needle scratches the skin of the fetus by accident, and a deep dermal wound is the consequence. The early embryo and fetus show an astonishing capability to re-epithelialize wounds rapidly. The edge of the wounded epidermis is smooth and under a circumferential tension. Basal epidermal cells are drawn forward by an actin cable acting as a contractile purse string [30]. Because the epidermal cells do not need to alter their integrins, as adult epidermal cells do, they can start moving promptly.

Mammalian embryos heal dermal skin wounds without scarring and with complete regeneration of the skin architecture in the first and second trimesters (Figure 4) [31]. A 1979 case report of intrauterine wound healing in a human fetus at 20 weeks first described this phenomenon [32]. The transition depends on both wound size and

gestational age [33, 34] and occurs near the end of the second trimester and beginning of the third trimester of gestation [35, 36]. Numerous intrinsic and extrinsic differences between fetal and adult wound healing have been suggested as possible explanations for this discrepancy. The transition from scar-free embryonic wound healing to scar-forming adult wound healing is gradual, and is characterized by dermal overdeposition of interstitial collagens, no regeneration of dermal appendages, a flattened epidermis, and differentiation of fibroblasts into myofibroblasts [34, 37-39].

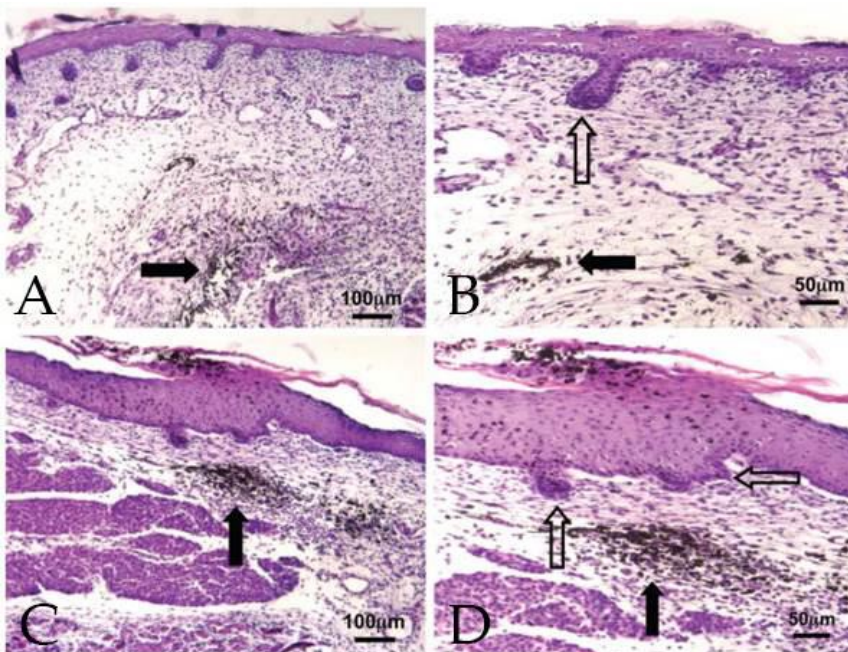


**Figure 4.** Scarless fetal wound healing occurs across species. The picture is showing scarless healing of fetal mouse wounds (hematoxylin and eosin staining). Black arrows indicate the India ink tattoo made at the time of wounding in order to demonstrate scarless wound location. (A and C) Healed wounds 72 hours after wounding. (B and D) Magnified views of the same wounds. Open arrows indicate epidermal appendages (developing hair follicles) within the wound site. No inflammatory infiltrate is present. Reproduced with permission from J Plast Reconstr Surg [33].

Fetal wounds differ from adult wounds in terms of their inflammatory responses, growth factor expression and responses, profile of gene expression, and ECM components [40]. The dermal ECM is composed primarily of collagen, elastic fibers, proteoglycans, and glycosaminoglycans. It is important for cell adhesion, differentiation, and proliferation, and serves as a reservoir for growth factors [41]. The fetal ECM differs from the adult ECM in terms of collagen composition, hyaluronic acid (HA) content, and proteoglycan ECM modulators, and these differences are thought to contribute to fetal scarless repair [37]. Several differences between fetal and adult dermal fibroblasts have also been defined. Fetal fibroblasts *in vitro* synthesize more total collagen and a higher proportion of collagen types III and IV than type I collagen in comparison to adult fibroblasts [14, 42]. Furthermore, fetal and adult fibroblasts differ in their expression of HA synthase in response to inflammatory cytokines [43], and fetal fibroblasts have two- to four-fold more surface HA receptors than adult fibroblasts [44]. The higher concentrations of HA and HA receptors are thought to enhance fibroblast migration and accelerate repair [45].

## Scaffolds, Tissue engineering, and Guided tissue regeneration of the skin

The loss or failure of tissues and organs is a frequent clinical problem in health care. In many cases, autologous transplantation is not possible and using allogenic donor tissue raises difficulties. Tissue engineering or guided tissue regeneration are used clinically to replace cells or tissues. For example autologous melanocytes are used to treat vitiligo [46] and carbon fibers formed to scaffolds can enhance ingrowth of regenerative tissue in patients with deep cartilage lesions [47].

The majority of all skin wounds heal spontaneously, but wounds that are deep dermal or full thickness may need special care and may benefit from regenerative materials [24, 48-52]. Guided tissue regeneration of the skin is used in burn care. A bilaminar membrane, in which the dermal portion is composed of bovine collagen and chondroitin-6-sulphate, is used in general practice as a skin substitute and dermal regeneration scaffold [53]. Another well-known dermal substitute is cell-free allograft dermis from cadavers [54].

In 1993, Langer and Vacanti defined tissue engineering (TE) as “an interdisciplinary field that applies the principles of engineering and the life sciences toward the development of biological substitutes that restore, maintain, or improve tissue function” [52]. The field of TE includes two fundamentally different methods. Autologous cells can be cultured *in vitro*, and transplanted back to the patient in a cell suspension, a graft, or in a three-dimensional biodegradable matrix as a carrier. Alternatively, regeneration could be stimulated *in situ* by implanting specially-designed materials or substances in a process called guided tissue regeneration [50, 55].

Guided tissue regeneration is achieved by designing the material so that only the desired types of cells enter the area and regenerate new tissue. In skin wound care, the scaffold ideally covers the wound initially, and as the regeneration takes place it is gradually degraded. Much scientific effort has been made to design dermal substitutes. New biomaterials are being developed, but no single scaffold has yet demonstrated all the desired qualities, such as inducing perfect regeneration, being well-tolerated, biodegradable as well as being easy storable, usable, and affordable [50, 53, 54, 56, 57].

## The fetal environment

A fetal cutaneous wound is submerged in amniotic fluid (AF), rich in nutrients and growth factors, and this environment may be essential to the properties of fetal wound healing [58-61]. The AF is a complex and dynamic biological fluid initially formed from the maternal plasma. Free diffusion occurs between the AF and the fetus across the fetal skin before the skin is gradually keratinized from 19 to 25 weeks of gestation. By 8 to 11 weeks of gestation, fetal urine is produced, and the fetus starts to swallow AF. Fetal urine is the major source of AF during the second half of pregnancy, and secretion by the fetal lungs is the second source. Water and solutes also move between AF and fetal blood within the placenta and membranes. AF contains; water, electrolytes, proteins, peptides, carbohydrates, lipids, and hormones, and the composition varies with gestational age [62, 63].

Human amniotic membrane, which surrounds the fetus and AF during pregnancy, has been used as an effective burn dressing since it was first introduced at the beginning of the last century [64-67]. The amniotic membrane prevents heat and water being lost from the surface of the wound, has low antigenicity, gives good pain relief, protects the wound from infection, and promotes rapid re-epithelialization and wound healing [68, 69]. Whether these qualities arise from the amniotic membrane or from exocrine activity of the amniotic cells is not fully understood.

## Hyaluronic acid

The ECM, which also differs between fetal and adult wounds, is known to play a role in regulating growth factors and cytokines and to alter cell behavior [70]. Fetal wounds demonstrate increased levels of glycosaminoglycans, such as HA, in the

ECM. HA is a high molecular weight polysaccharides found on the cell surface or in the ECM [71, 72]. The concentration of HA is increased during embryogenesis, tissue proliferation, regeneration, and repair. Unique to fetal wounds is that the concentration of HA remains high through the entire healing process and that fetal fibroblasts express higher levels of HA receptors than adult fibroblasts [73, 74]. During the second trimester, AF displays high concentrations of HA [75], and AF also stimulates endogenous HA synthesis in fetal skin [76]. Hyaluronidase [77], one of the enzymes that degrades HA, is expressed in much higher amounts in adult wound fluid than in fetal wound fluid, which may be one reason for the greater deposition of HA in fetal wounds [78]. Addition of HA-rich matrices is known to reduce scar formation in adults [79].

## Wound models and Wound-healing measurements

When studying the wound-healing process, there is a need for standardized, well-established, and reproducible *in vitro* and *in vivo* wound-healing models. Different models have different benefits and limitations as well as associated costs and ethical considerations. The following sections present examples of selected models.

### CELL CULTURE

Cell culture of different cell types, cultured separately or in co-culturing systems, allows the study of specific cell responses to different factors. Cell culture is widely used and is readily available but sometimes represents a too simplified method. One of the simplest models is the monolayer scratch wound. By altering the environment, the cells, or the media, researchers can study different effects of the stimuli [80, 81].

### THREE-DIMENSIONAL *IN VITRO* MODELS

More complex three-dimensional structures can mimic the *in vivo* situation and are highly reproducible; however they do not allow the researchers to study the whole body response and lack a complete immune system. Simpler models of wound healing allow studying of specific parts of the wound-healing process [82]. Wound repair within the dermis can, for example be studied by introducing fibroblasts into a solution of collagen [83, 84]. To study the interaction between dermal and epidermal cells, keratinocytes could be cultured on a collagen matrix [85] or a skin punch biopsy could be fixed onto acellular dermis [86].

### THE SKIN BLISTER MODEL

Superficial wounds (8mm  $\emptyset$ ) are created *in vivo* by applying vacuum pressure to a fenestrated plastic template. The epidermal part of the blister is removed, and a plastic well is positioned over the wounds. This model allows collection of wound exudate during re-epithelialization and study of the inflammatory phase [87].

### SKIN BIOPSY MODELS

Circular discs of full-thickness wounds are created under local anesthesia in the skin or oral hard palate with a biopsy punch. The skin biopsy procedure is minimally invasive. The method is easily repeatable and creates a wound with tissue loss. This approach allows researchers to measure re-epithelialization, dermal reconstruction, and wound contracture by processes such as visual inspection, photo planimetry, or ultrasound scanning [88-91].

### VISUAL INSPECTION AND IMAGING

Visual inspection is the clinical gold standard for measuring wound healing. Photographing allows non-invasive serial measurements, and high-resolution images of the wounds can be used to identify epithelial growth at the wound margins [92]. Ultrasound scanning permits quantitative measurements of structural tissue changes

within the wound, and the wound margins are more easily identified compared with photographing; however ultrasound does not record the wound's appearance [93]. Laser Doppler flowmetry and tissue viability imaging (TiVi) are non-invasive methods to measure the cutaneous circulation and red blood cell concentration, respectively [94, 95].

#### **SURFACE AREA MEASUREMENTS**

Physicians, nurses, or researchers often use different techniques to measure the wound area of chronic wounds. The simplest way is to measure the two maximal perpendicular dimensions of the wound with a ruler [96]. Wound tracing is more precise and considered the gold standard for measuring wound size. A transparent film is placed over the wound, and the wound perimeter is traced with a marker. The weight of the transparent film, representing surface area, can be recorded.

#### **ANIMAL MODELS**

Animal models are often used for wound studies in order to enable study of the systemic pathophysiology of an injury [97]. However, variations exist in the structure and anatomy of the skin of different species. For example, the mouse and rat skin has thinner epidermis and dermis and more dense hair with shorter hair cycle in comparison to humans. Murine skin, like the skin of other quadrupeds, has a thin skeletal muscle layer, the *panniculus carnosus*, that is only found in the platysma of the neck in humans [98]. Pig skin closely resembles that of humans, and wound healing undergoes the same phases, but the pattern of vascularization differs in some aspects. Pigs have a greater risk of infections than smaller animals and demand more extensive care [99, 100].

#### **WOUND MODELS USED IN THIS THESIS**

In this thesis, we have implanted a dermal substitute by incision or injection and biopsied full thickness skin with the implant included for analysis. We have also

used an earlier described and, in our research group, well-used *in vitro* wound model in human donor skin. This model allows standardized, highly reproducible, multiple skin wounds to be studied for re-epithelialization and dermal regeneration following different interventions [101]. Further on, we have developed an earlier described minimally invasive *in vivo* wound model [102]. In this process, we produced standardized deep dermal wounds with blood collection lancets and analyzed the wounds by tissue viability imaging, histology and proteomics.



# Aims of the Thesis

Most cutaneous wounds heal within a week or two, but the result is neither visually nor functionally perfect. Even though epidermis regenerates, the process results in a connective tissue scar with dense parallel bundles of collagen, instead of the fine meshwork of unwounded dermis. A central goal with studies on skin wound healing is to explore how skin can be stimulated to reconstruct the tissue damage better and reach complete regeneration. The wound-healing process has been explored in Papers I-IV, and each has its specific objectives.

## Specific aims Papers I-IV

- How can we improve wound healing by developing and using new dermal substitutes? Can dermal repair be turned into regeneration?

(Papers I and II)

- What role does hyaluronic acid play in the wound-healing properties of amniotic fluid, and can human adult wound healing be altered by exogenous hyaluronic acid?

(Papers III and IV)

- Can tissue viability imaging, histology, and proteomics be combined to study wound healing in a further developed, earlier described, minimally invasive human *in vivo* wound model?

(Paper IV)



# Material and Methods

## Cell culture (Paper I)

For Paper I, we obtained human dermal fibroblasts from normal human skin that had been donated by healthy patients having routine plastic surgery. Subcutaneous fat and epidermis were removed as much as possible by scissors. Subsequently, the remaining dermis was divided with scissors into small fragments and enzymatically digested. Tissue suspension was triturated repeatedly with a pipette to dissociate tissue fragments and centrifuged at 400 g for 10 minutes. The supernatant was removed, and the cell pellet re-suspended in culture medium. The cells were further cultured in culture flasks for numerical expansion.

For the *in vitro* experiments in Paper I, fibroblasts from one donor and of the third generation were used. Scaffolds, 2 mm thick, were cut to 2 cm<sup>2</sup> circular discs and left to soak for 24 hours in fibroblast culture medium in 24-well culture plates. The medium was then removed and the scaffolds were seeded with  $1 \times 10^5$  fibroblasts in 1 ml culture medium/well.

## Scaffold materials (Papers I and II)

### POLY(URETHANE UREA) (PAPER I)

The poly(urethane urea) (PUUR) scaffolds were synthesized in solution using a two-step polymerization method first described by Gisselält et al. [103]. Four different types of scaffolds were used, one fibrous and three porous (Table 1 and Figure 5). All scaffolds were sterilized by electron beam irradiation (28 kGy).

Sample code	Soft segment	Hard segment	Study
<b>Fibrous scaffold</b>	PDEA 550	MDI:1,2-DAP	<i>in vitro</i>
<b>Porous scaffold</b>	PCL 530	MDI:1,3-DAP-2OH	<i>in vitro</i>
<b>Scaffold A (12%, Artelon®)</b>	PCL 530	MDI:1,3-DAP	<i>in vivo</i>
<b>Scaffold B (9%, Artelon®)</b>	PCL 530	MDI:1,3-DAP	<i>in vivo</i>

**Table 1.** Chemical composition of scaffolds used in the various parts of the study. PDEA: poly(di(ethylene glycol) adipate); PCL: polycaprolactone diol; MDI: 4,4'-diphenylmethane diisocyanate; 1,2-DAP: 1,2-diaminopropane; 1,3-DAP: 1,3-diaminopropane ; 1,3-DAP-2OH: 1,3-diamino-2-hydroxypropane.

For the fibrous scaffold, a 30% w/w polymer solution was extruded through a spinneret (120 holes, diameter 80  $\mu\text{m}$ ) and coagulated in hot water (80  $^{\circ}\text{C}$ ) to form fibers that could be packed in a cylindrical mold (12 mm  $\varnothing$ ). A solution of 92% N, N-dimethylformamide (DMF) and 8% water was allowed to pass through the packed

fibers, binding them together. The fibrous scaffold was then washed with water, dried, and sliced into discs 2 mm thick.

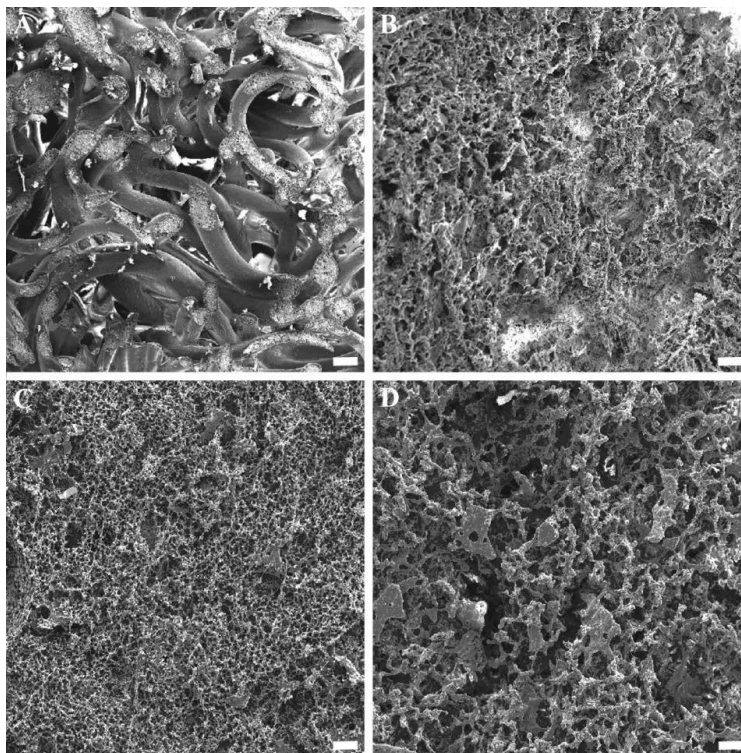


**Figure 5.** Scanning electron micrographs of the different scaffolds used. (A) Fibrous scaffold, *in vitro* study. (B) Porous scaffold, *in vitro* study. (C) Scaffold A, *in vivo* study. (D) Scaffold B, *in vivo* study. The fibrous scaffold had larger pores ( $\sim 600 \mu\text{m}$ ) and a more irregular structure than the scaffolds produced by the solvent casting/particle leaching process. The porous scaffolds had a similar appearance even though there were differences in concentrations of polymer and sugar, and in the size of the particles (bars =  $100 \mu\text{m}$ ).

For the porous scaffolds, a solvent casting/particle leaching process was used. The polymer solution was in this case diluted with DMF to a concentration of 9% w/w or

12% w/w. The 12% w/w solution was mixed with glucose in a ratio of 33:40 for the porous scaffold used in the *in vitro* studies. For the *in vivo* part of the study, two kinds of porous scaffolds were selected and tested. For the porous scaffold A, sieved glucose monohydrate (particle size 150 to 250  $\mu\text{m}$ ) was mixed with 12% w/w polymer solution, and for the porous scaffold B, un-sieved glucose monohydrate (particle size  $\sim$ 10-500  $\mu\text{m}$ ) was mixed with 9% w/w solution. The resulting mixture formed a gel that was soaked in a water bath at 40  $^{\circ}\text{C}$  to remove the glucose and DMF. The washing was continued until the weight of the dried scaffold was constant. The scaffolds were then sliced into discs 2 mm thick.

### MACROPOROUS GELATIN SPHERES (PAPER II)

The gelatin spheres (CultiSphere-S, Percell Biolytica AB, Åstorp, Sweden) were based on a highly cross-linked type A porcine-derived gelatin matrix (Figure 6) [104]. The spheres had an outer diameter of 70-170  $\mu\text{m}$  and an internal pore size of 10-20  $\mu\text{m}$ .

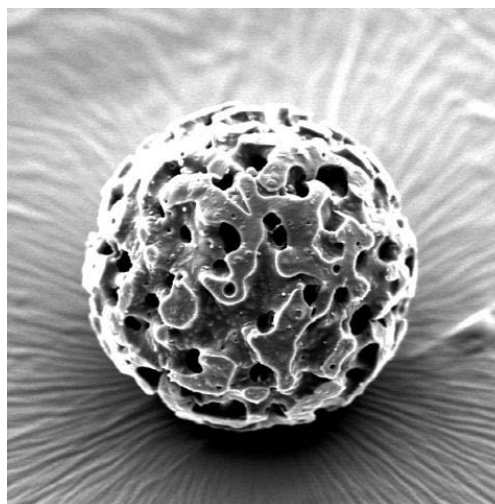


**Figure 6.** Scanning electron microscope image of a porous gelatin sphere with a diameter of 166-370  $\mu\text{m}$  and an average internal pore size of approximately 30  $\mu\text{m}$ .

Image captured by Sofia Pettersson.

All gelatin spheres were prepared according to the manufacturer's instructions. In summary, dry gelatin spheres were rehydrated for a minimum of one hour at room temperature in calcium-free and magnesium free phosphate buffered saline (PBS), 50 ml g<sup>-1</sup>. The solution of gelatin spheres and PBS was sterilized by autoclaving and stored at 4 °C. Before use, the spheres were washed twice in fresh PBS, let to sediment to the bottom of a test tube, and were then aspirated with a 1 ml syringe. A total amount of 0.8 ml suspension was aspirated. The syringe was turned upside down for sedimentation for 30 minutes, and the "supernatant" was removed, leaving 0.5 ml densely packed gelatin spheres in the syringe to use for injection.

## Culture conditions (Papers I and III)

Cell and wound cultures were incubated at 37 °C, 5% carbon dioxide, and 95% humidity. During the numerical expansion of cells, morphological inspection was performed when the medium was changed.

## Culture media (Papers I and III)

### FIBROBLAST CULTURE MEDIUM (PAPER I)

- Dulbecco's Modified Eagle's Medium (DMEM) supplemented with 10% newborn calf serum (NCS)

### WOUND CULTURE MEDIA (PAPER III)

- 100% DMEM
- 90% DMEM supplemented with 10% fetal calf serum (FCS)
- 50% DMEM supplemented with 50% FCS
- 90% DMEM supplemented with 10% amniotic fluid (AF)
- 50% DMEM supplemented with 50% AF
- 50% DMEM supplemented with 50% AF and added hyaluronidase (20 IU/ml)
- 50% DMED supplemented with 50% FCS and added hyaluronidase (20 IU/ml)

All culture media contained antibiotics (penicillin 50 U/ml and streptomycin 50 µg/ml) and were changed every second or third day. Each culture-well contained 1 ml culture medium. The hyaluronidase was prepared according to the manufacturer's instructions.

### Collection of human amniotic fluid

After signed informed consent from the patients, residual human AF was obtained from ultrasound-guided amniocenteses from women who were 14-18 weeks' pregnant. The fluid from approximately 100 patients was pooled centrifuged at 2400 g for 5 minutes. The supernatant was put through a sterile filter before use.

## *In vitro* wounds and Wound culture (Paper III)

Skin was obtained from healthy women having routine breast reduction. In Paper III, skin from three donors was used. Standard wounds were produced at the laboratory as previously described by Kratz et al. (Figure 7) [101, 105].

Samples were transferred to 24-well cell culture plates containing culture media, and they were placed with the epidermal side up. The groups contained eight wounds/time point (DMEM, 10% FCS, 10% AF, and 50% AF), four wounds/time point (50% AF or 50% FCS with added hyaluronidase), or 12 wounds/time point (50% FCS).

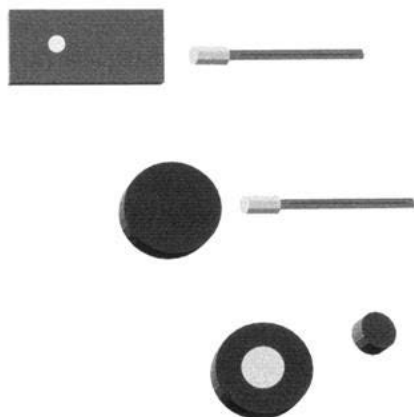


**Figure 7.** Wounds were produced using circular discs of skin cut with a 6-mm biopsy punch. In the center of each sample, on the epidermal side, a deep dermal wound was created with a 4-mm biopsy punch and scissors (~1 mm deep) as earlier described. All wounds were examined histologically regarding depth, and no adnexal structures for epidermis to regenerate from were seen.

## Routine histology (Papers I-IV)

The specimens were fixed overnight in 4% neutral buffered formaldehyde, washed in PBS, and dehydrated through an ethanol-xylene series (70% ethanol - overnight, 95% ethanol - 2 hours, 99.5% ethanol - 2 hours, and xylene - 30-60 minutes). Dehydrated samples were soaked in warm liquid paraffin. After cooling sections, 7-10  $\mu\text{m}$  thick, were cut with a microtome and transferred to a warm water bath. Then they were placed on microscopy glass slides, deparaffinized, rehydrated, and stained with hematoxylin and eosin before being examined under a light microscope and photographed.

In Paper III, vertical sections from the center of the wounds, including intact epidermis and a central deep dermal wound, were mounted, and images were captured. Re-epithelialization was measured in the digital images by two independent and blinded observers (Figure 17). Repeated measurements were made, and re-epithelialization was expressed as percentage of epithelialized length over total wound length. The mean value from the two observers was used for statistical analysis.

In Paper IV, the biopsies were orientated so that vertical sections of the wounds were generated including the epidermis and a deep dermal central wound. Two independent observers, one of which was blinded, determined re-epithelialization using light microscopy. Only a complete re-epithelialization was regarded as a positive result. The dermis was also examined regarding the morphology and presence of cells.

## Immunohistochemistry (Papers I and II)

Samples from the *in vitro* and *in vivo* experiments in Paper I were stained immunohistochemically for deposition of pro-collagen, indicating actively-secreting fibroblasts. A monoclonal rat-anti-human antibody raised against pro-collagen was used as the primary antibody. Samples from the *in vivo* experiments in Paper I were also stained for endothelial cells with monoclonal mouse-antihuman von Willebrand factor indicating angiogenesis and re-vascularization as well as monoclonal mouse-antihuman CD68 antibody to detect macrophages and granulocytes.

In Paper II, samples were stained immunohistochemically for endothelial cells using the same primary antibody as in Paper I.

A biotinylated anti-IgG antibody was used as the secondary antibody. After washing in PBS, bound antibodies were localized with avidin- peroxidase Vectastain Elite ABC kit, and the substrate was an avidin-horseradish peroxidase complex, Vector® VIP. Negative controls were established by omitting the primary antibody.

## Subjects (Papers I, II, and IV)

For Papers I, II, and IV, healthy male volunteers were recruited according to inclusion and exclusion criteria (Table 2 and 4). A physical examination was made, and blood samples were taken at the beginning and at the end of the studies.

### PAPER I

Four healthy volunteers were recruited, aged 30 to 42 years (mean 34). The upper part of the right or left buttock was used as the study site in all subjects. A case report form was set up for each participant, and the study period was eight weeks.

After washing the skin with chlorhexidine solution and injecting local anesthetic, six intradermal pockets were created in each subject using a 4-mm biopsy punch and scissors. The relative locations of scaffolds and control sites were decided by pre-made randomized templates; two discs at a size of 4 mm in diameter and 2 mm thick of each scaffold (scaffold A and B) were inserted. Two pockets (the control sites) were left without insertion of scaffolds. The pockets were photographed, closed with wound tape, and covered with permeable non-woven tape.

The study sites were photographed (Figure 8) every seventh day according to the plan of assessments (Table 3). Changes such as swelling, heat, redness, purulent secretion, blistering, and eczema as well as any adverse events such as for example itching, pain, or other subjective symptoms were noted. The study sites were again covered with a permeable non-woven tape.

After two and eight weeks one of each implant (A and B) and one control (C) were removed, after washing with chlorhexidine and administration of local anesthetic, with a 6 mm biopsy punch. The wounds were closed with wound closure tape.

Inclusion criteria	Exclusion criteria
<ul style="list-style-type: none"> <li>• Healthy volunteers</li> <li>• Male</li> <li>• Age between 18 and 50 years</li> <li>• Signed informed consent</li> </ul>	<ul style="list-style-type: none"> <li>• Underlying severe disease or other disease judged by the investigators to interfere with the study</li> <li>• Previous inclusion in another study within the last three months</li> <li>• Scar tissue at the site of the surgical incision</li> </ul>

**Table 2.** Inclusion and exclusion criteria for Papers I and II.

Visit	1	2	3	4	5	6	7	8	9
Day	0	7	14	21	28	35	42	49	56
<b>Variable</b>									
Physical examination	X								X
Insertion of scaffold	X								
Biopsy			X						X
Laboratory examination	X								X
Picture	X	X	X	X	X	X	X	X	X
Skin signs/Symptoms	X	X	X	X	X	X	X	X	X
Adverse events		X	X	X	X	X	X	X	X

**Table 3.** Plan of assessments Paper I.



**Figure 8.** Photograph of study site two weeks after insertion of scaffolds. There is protrusion of the scaffolds, and slight redness can be seen. (C1: control to be removed after two weeks; C2: control to be removed after eight weeks; A1: scaffold A to be removed after two weeks; A2: scaffold A to be removed after eight weeks; B1: scaffold B to be removed after two weeks and B2: scaffold B to be removed after eight weeks).

## PAPER II

Eight healthy volunteers were recruited, aged 24 to 38 years (mean 28). The ventro-medial aspect of the upper arm was used as the study site in all subjects.

One week before injections, a 1-mm dot was tattooed on the planned injection points, using tattoo ink. A case report form was set up for each participant, and the study period was 9 or 27 weeks (subjects were included one week before injections at the same visit as the tattooing).

After washing the skin with 70% alcohol and injecting local anesthetic, the intradermal injections were given. Each subject was given eight injections with a 27-gauge/0.4-mm  $\varnothing$  needle; two injections with saline solution, two with Restylane®/2% cross-linked, non-animal derived HA, and four injections with gelatin spheres. A volume of 0.5 ml of each solution was given (Figure 9). The relative localization of different injections was decided by pre-made randomized templates.



**Figure 9.** Photograph of the injection sites one week after injection. (C: control, R: Restylane®/cross-linked hyaluronic acid, and MGS: macroporous gelatin spheres).

Every seventh day, the study sites were photographed. Any changes such as swelling, heat, redness, purulent secretion, blistering, or eczema were noted and so were any adverse events such as itching, pain, or other subjective symptoms.

The subjects were divided into two groups (four per group). Subjects in group 1 had one of each injection/implant removed after two weeks and one after eight weeks. For group 2, the injections/implants were removed after 12 and 26 weeks respectively. Removal of implants was done after washing the skin with 70% alcohol and administering local anesthetic. A 6-mm biopsy punch was used to remove a full thickness skin biopsy including the implant and surrounding tissue. The wounds were closed with stitches and wound closure tape.

#### PAPER IV

Ten healthy volunteers between 20 and 27 years of age (mean 23) were enrolled in the study (sample size was based on an 80% power calculation). Biopsies from subjects with blood sample results outside the reference intervals were excluded from the proteomics analysis, and their results were not included in statistical comparisons regarding results from tissue viability imaging (TiVi) and re-epithelialization. Left proximal ventral forearm skin was used as the study site and had to be uninjured and scar free. A case report form was set up for each participant, and the study period was 14 days (Table 5).

Randomization of location of treatments was carried out by drawing lots; after washing the skin with chlorhexidine, four sites on each subject were pre-treated with an intradermal injection of 0.05 ml HA (Hyalgan®/natriumhyaluronat 10 mg/ml), and four additional sites were injected with 0.05 ml saline solution. For the remaining four sites on each subject, a sham injection was administered where the needle was introduced intradermally, but no injection was given. Injections were made entering the skin from the side with a U-100 insulin 29-gauge/0.33-mm  $\varnothing$  needle approximately 8 mm from the planned wound.

Inclusion criteria	Exclusion criteria
<ul style="list-style-type: none"> <li>• Healthy volunteers with no medications</li> <li>• Male</li> <li>• 18 – 40 years old</li> <li>• Signed informed consent</li> </ul>	<ul style="list-style-type: none"> <li>• Impaired health or regular medications</li> <li>• Impaired wound healing and/or abnormal response to minor skin trauma</li> <li>• Previous inclusion in another study within the last three months</li> <li>• Nicotine use</li> </ul>

**Table 4.** Inclusion and exclusion criteria for Paper IV.

Visit	1	2	3	4	5	6	7	8	9	10	11	12	13	14
Day	0	1	2	3	4	5	6	7	8	9	10	11	12	13
<b>Variable</b>														
Informed consent	X													
Physical examination	X													X
Blood sample	X													X
Photography	X	X	X	X	X	X	X	X	X	X	X	X	X	X
Incision	X													
Biopsy		X												X
Unexpected skin reactions	X	X	X	X	X	X	X	X	X	X	X	X	X	X
Adverse events	X	X	X	X	X	X	X	X	X	X	X	X	X	X

**Table 5.** Plan of assessments Paper IV.

Twelve deep dermal standardized wounds were created in each subject with single-use spring-loaded sterile blood collection lancets. The wounds were made with a depth of 1.6 mm and a width of 1.8 mm by pressing the lancet gently against the skin and releasing the trigger. For the wounds where a prior injection had been given, the

lancet was centered over the weal. A swab soaked in saline solution was held over the site for five minutes to minimize bleeding and crust formation. The subject stayed for one hour for observation, and any skin reactions or adverse events were noted. After one hour had passed, the study area was photographed with TiVi. The study site was left without dressing, and subjects were asked not to expose the study site to friction, for example by rubbing after taking a shower.

After 24 hours and at 14 days, the skin was washed with chlorhexidine and injected with 10 ml of local anesthetic proximal to the study sites. At each time point, seven biopsies were taken at the following sites: two wounds injected with HA (named "HA1" and "HA13" respectively), two wounds injected with saline solution ("NaCl1" and "NaCl13"), two wounds that had a sham injection ("untreated wound1" and "untreated wound13"), and one sample of normal, unwounded skin ("unwounded skin1" and "unwounded skin13"). For the biopsies 2-mm biopsy punches were used. The wounds were closed with a stitch and wound closure tape. A compressive dressing was put around the forearm to minimize bleeding and hematoma. The subjects were asked to remove the external dressing after one hour.

## Tissue viability imaging (Paper IV)

To visualize the cutaneous microcirculation, TiVi was used (Figure 10) [106, 107]. The camera was positioned 30 cm directly above the study area, and photographs were taken every day for a period of 14 days. The mean TiVi value for each region of interest (ROI), 3-mm  $\varnothing$ , was generated and exported to Microsoft Excel for further calculations and analysis. To show only relative changes in erythema intensity, the mean TiVi-value from the undamaged skin was subtracted from mean TiVi values generated from the ROIs encircling the incisions. Mean TiVi index values were

pooled according to treatment (HA, NaCl, untreated wound) and analyzed on a group basis. All measurements were done at a constant room temperature of 23 °C.

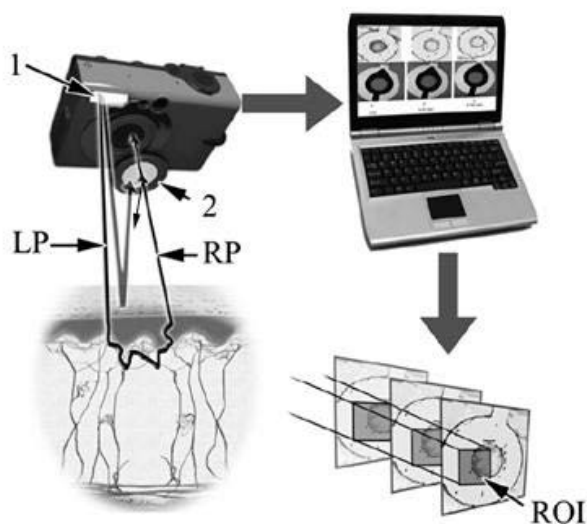


**Figure 10.** Quantification of red blood cell concentration in the cutaneous microcirculation by use of a tissue viability imaging (TiVi) system. Utilization of polarized light [106] can illustrate temporal [107] as well as spatial changes in red blood cell concentration. Light from the flash is linearly polarized by the first filter (1). A portion of the light is directly reflected from the surface of the skin, retaining its polarization and is stopped by the second filter in front of the lens (2). A part of the light penetrates the tissue and is scattered. When re-emitted from the skin surface the light has been randomly polarized and some of it can pass through the second filter. The wavelength dependent difference in absorption of the red blood cells is utilized by the software to generate numerical values (TiVi values) and color-coded two-dimensional maps of the concentration of red blood cells. TiVi data was acquired using a standard digital camera with an illuminator for continuous illumination. Mean TiVi value data for each region of interest region of interest (ROI) was generated using the built-in analysis feature of the WheelsBridge software. (LP: linearly polarized and RP: randomly polarized).

## Proteomics (Paper IV)

Biopsy samples were heat stabilized with Denator Stabilizer and stored at  $-20\text{ }^{\circ}\text{C}$  until further analysis. Subsequently, the biopsies were placed in Eppendorf tubes, and  $300\text{ }\mu\text{l}$  of sample solution (9 M Urea, 4% 3-((3-cholamidopropyl) dimethylammonio)-1-propanesulfonate (CHAPS) (w/v), 65 mM Dithiothreitol (DTT), 2% Pharmalyte 3-10 (v/v), trace of bromophenol blue) was added. The samples were then homogenized by sonication  $3 \times 10$  seconds, incubated for two hours at  $4\text{ }^{\circ}\text{C}$ , and finally centrifuged at  $20\,000\text{ g}$  for one hour.

The protein concentration was measured in each sample using a Quant kit according to the manufacturer's recommendation. An aliquot of  $15\text{ }\mu\text{g}$  of protein from each nine of the subjects were pooled into eight groups according to sample. Of the resulting pooled samples  $100\text{ }\mu\text{g}$  were analyzed by two-dimensional gel electrophoresis (2-DE) in a horizontal setup (IPGphor and Multiphor) essentially according to Görg [108]. The separated proteins were stained with silver [109], and the protein patterns were analyzed as digitized images, using a charged-coupled device camera (CCD camera) in combination with a computerized imaging 12-bit system designed for evaluation of 2-DE patterns as previously described [110]. Spots were matched, and the amount of protein in a spot was assessed as background corrected optical density, integrated over all pixels in the spot and expressed as integrated optical density. In order to correct for differences in intensity between different 2-DE images, the amounts of the compared protein spots were quantified as optical density for individual spot per total protein intensity of all spots in the same gel.

Protein spots were excised from the 2-DE gel and digested with trypsin. The dried tryptinized samples were dissolved in  $6\text{ }\mu\text{L}$  of 0.1% formic acid. Peptides were analyzed using an online nano-flow High Performance Liquid Chromatography

(HPLC) system (EASY-nLCII) in conjugation with a mass spectrometer. Obtained data files were analyzed by Proteome Discoverer 1.4, and the search algorithm SEQUEST was used against UniProt release 2013\_09 Homo sapiens database. Carbamidomethylation of cysteine residues was set as the static modification, and oxidation of methionine was set as the variable modification. The precursor mass tolerance was set to 10 ppm with 0.6 Da fragment mass tolerance. Proteins were identified with a minimum of two peptides of rank 1 with high score and target false discovery rate 0.01.

## Statistics

In Paper III, statistical comparisons of re-epithelialization were made using non-parametric Kruskal-Wallis tests with Dunn's multiple comparison post-tests. Statistical comparisons of scoring of re-epithelialization in Paper IV were made using non-parametric McNemars test. Probabilities of less than 0.05 were accepted as statistically significant. Statistical analyses were made using GraphPAD Prism 5.0.

Mean TiVi values in Paper IV were arranged into three arrays according to groups (HA, NaCl, and untreated wounds) of 18 columns (ROIs) and 16 rows (time points). A mean for every row was calculated and plotted (Figure 20), and the difference in effect of treatment on the erythema intensity was calculated using repeated measures ANOVA.

The proteomic data in Paper IV was analyzed using a multivariate projection model, Orthogonal Partial least squares regression (OPLS) with discriminant analysis (DA) [111] to find a relationship between spot volume ratios and a binary Y vector by

using class membership data. The spot volume ratios were mean centered and scaled for unified variance using SIMCA-P+ v.13.0.

## Ethical approvals and Ethical considerations

All studies were performed after approval by the local Ethics Committee.

**PAPER I** The study was approved by the local Ethics Committee at Karolinska Institutet, Stockholm, Sweden (register number 01-114) and the Swedish Medical Products Agency (register number 34:2001/3692) and was performed according to the Declaration of Helsinki of 1964, as revised in 1983.

**PAPER II** The study was approved by the local Ethics Committee at Karolinska Institutet, Stockholm, Sweden (register number 03-172) and the Swedish Medical Products Agency (register number 461:2003/69076) and was performed according to the Declaration of Helsinki of 1964, as revised in 1983.

**PAPER III** The study was approved by the local Ethics Committee at Linköping University, Sweden (register number 03-342) and was performed according to the Declaration of Helsinki of 1964, as revised in 1983.

**PAPER IV** The study was approved by the local Ethics Committee at Linköping University, Sweden (register number 2013/371-31) and was performed according to the Declaration of Helsinki of 1964, as revised in 2013.

All subjects that participated in Papers I, II, and IV gave signed informed consent. The subjects were recruited by advertisements, and had no health care relationship to the researchers. The subjects volunteered, without being persuaded, and were informed that they could exit the study at any moment without any explanation required. Only a reasonable amount of financial compensation was given. All biopsies and study areas were intended to be as small as possible, to minimize scarring to the subjects. Study areas were chosen carefully to be located in hidden locations of the body. Administration of local anesthetics, tattooing dots, and performing the wound manoeuvre resulted in expected transitional pain. All *in vivo* studies followed earlier *in vitro* and/or animal studies within the same field of research.

For Papers I and III, skin was obtained from healthy women, having routine plastic surgery.

The AF used in Paper III was obtained from routine ultra-sound guided amniocenteses. The women were informed about the study by a written advertisement in the gynecologists' waiting room, and were asked for their participation in the study by the gynecologists, without any persuasion. No financial compensation was given and participation did not influence the health care in any way. The women gave signed informed consent. The AF was residual and no extra amount of fluid was collected due to the study. The AF was received at the laboratory without any labeling regarding personal data. The AF was pooled before

usage. No analysis of the AF was done and residual AF was discarded at the end of the study. Only the effect on wound healing of the pooled AF was studied.



# Main Results and Discussion

## Paper I

In the *in vitro* part of the study, fibroblast-like cells grew onto and into both the porous and the fibrous scaffold. The number of cells increased with time, and after six weeks production of pro-collagen was shown by immunohistochemical staining (Figure 11). No difference in ingrowth of cells or production of procollagen between the materials was seen, and the PUUR was judged as a suitable scaffold for human dermal fibroblasts.

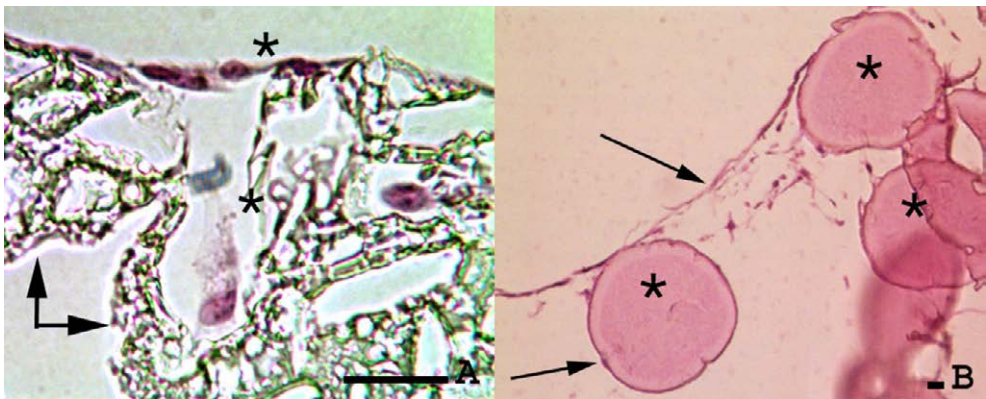


**Figure 11.** Immunohistochemical staining with monoclonal rat-antihuman pro-collagen I antibody of *in vitro* culture of human fibroblasts on scaffolds. (A) Porous scaffold indicated by arrows. Asterisks show the pro-collagen. (B) Fibrous scaffold indicated by asterisks and pro-collagen by arrows (bars = 10  $\mu\text{m}$ ).

The porous PUUR scaffold was considered more suitable for clinical applications and has also been studied for other clinical uses [112, 113]. The implants were well-tolerated, and all subjects completed the investigation. Two subjects reported itching during the study period, but they reported no difference between test and control sites. Besides the itching, no adverse events were reported, and all laboratory results were within reference ranges, both at the beginning and end of the study. Clinically there was slight redness around all incisions. Swelling, warmth, and minor turbid secretion were noted only around the test sites, and the skin covering the scaffolds partly contracted, resulting in some protrusion of the scaffolds. Scaffold B seemed to give more contraction of the skin lid and more obvious signs of inflammation. The inflammation around the scaffolds was expected as a foreign material always induces a certain reaction.

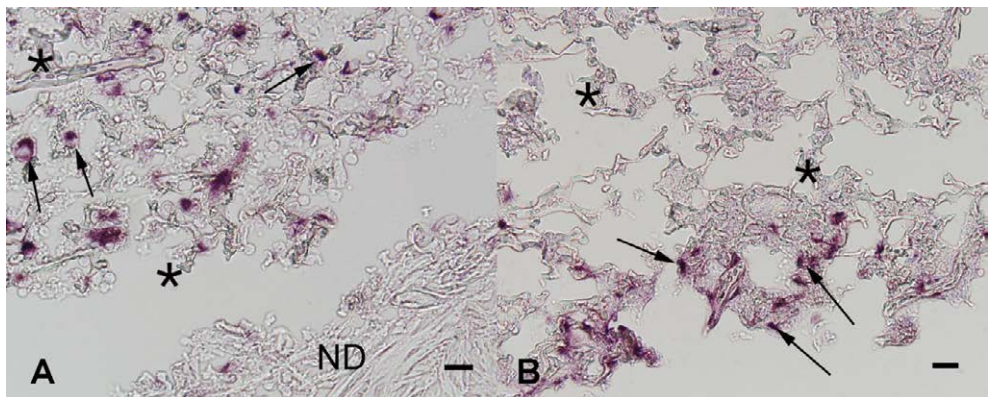


**Figure 12.** Immunohistochemical staining with monoclonal mouse anti-human CD68 antibody after two (A) and eight (B) weeks. Arrows show inflammatory cells present in the scaffold close to normal dermis (ND). Asterisks indicate the PUUR scaffold (bars = 10 $\mu$ m).

After two weeks, histological examination of the scaffolds showed ingrowth of a large number of cells, indicated to be neutrophils and macrophages by immunohistochemical staining (Figure 12). The controls showed normal healed skin with few inflammatory cells after two weeks. After eight weeks, the inflammatory cells had decreased in number in the scaffolds except for one subject that probably had a delayed inflammatory reaction, with fewer inflammatory cells at week two compared to week eight.

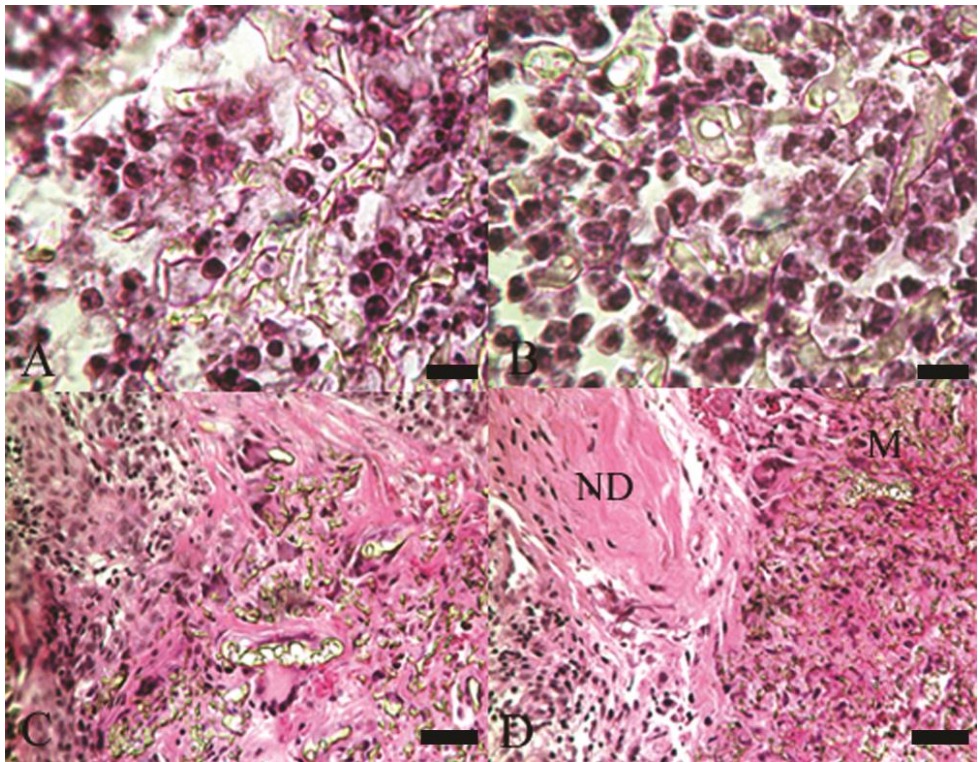


**Figure 13.** Hematoxylin and eosin staining of scaffolds from the *in vivo* part of the study. (A) Scaffold A after two weeks. (B) Scaffold B after two weeks. Scaffolds were completely occupied by cells, mainly inflammatory cells (bars = 10  $\mu\text{m}$ ). (C) Scaffold A after eight weeks. (D) Scaffold B after eight weeks. Fewer inflammatory cells were seen, and fibroblasts were growing in the entire scaffold. (ND: normal dermis and M: matrix/scaffold (colored greenish) (bars = 50  $\mu\text{m}$ ).

Spindle-shaped cells, considered to be ingrowing fibroblasts, were noted to some extent after two weeks. After eight weeks, they were growing in thick bundles and were occupying the entire scaffolds (Figure 13). Pro-collagen could be detected in two scaffolds after two weeks and in all scaffolds after eight weeks. A crucial parameter regarding regeneration of dermis is that the newly regenerated dermis is vascularized to allow transplantation of an epidermal transplant [24]. At two weeks, a few endothelial cells could be identified by immunohistochemical staining for von Willebrand factor, and after eight weeks capillary budding or ingrowth of capillaries was seen (Figure 14).

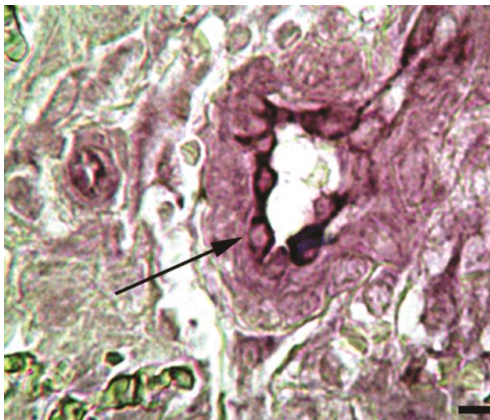


**Figure 14.** Immunohistochemical staining for von Willebrand factor/endothelial cells after eight weeks using a monoclonal mouse-antihuman von Willebrand factor in the poly(urethane urea) scaffold indicates vascularization. Arrow shows lumen of a capillary (bar = 10  $\mu\text{m}$ ).

The PUUR scaffold has previously been tested and has shown to have a degradation time of several years (unpublished data). A long degradation time might be beneficial as the scaffold then upholds the physical properties of dermis and slow degradation time leads to slower release of possible irritating degradation products. In this study, the subjects were healthy, and the scaffolds were surrounded by normal dermal tissue. Clinically, for example after a burn injury, the number of

normal dermal fibroblasts and endothelial cells may be reduced, further supporting the prolonged need for reinforcement of the wound by the scaffold.

Synthetic biomaterials can be bioengineered to match specific demands and can be tailored to specific applications. A synthetic polymer, like the PUUR scaffold, is manufactured with a high degree of reproducibility and minimal risk of contamination. The PUUR scaffold used in this study (Artelon®, Artimplant AB, Göteborg, Sweden) has already been used clinically for anterior cruciate ligament reconstruction and as a degradable trapeziometacarpal spacer [112, 113]. Long time clinical data and biopsy specimens from patients demonstrate that the material is highly biocompatible [113]. The PUUR scaffold degenerates by hydrolysis and has not shown to induce induction of any chronic inflammation or foreign body giant cell granulomas [113].

The initial result from using the PUUR scaffold for dermal regeneration indicates that the scaffold could function as a dermal substitute. However, in the present study, the scaffolds were small and the study period relatively short. Further studies with larger standardized wounds and clinical studies on burn patients are necessary to evaluate the clinical values. A larger scaffold would give the opportunity to biopsy more frequently and to follow the ingrowth of cells over time.

In conclusion, the PUUR scaffold was well-accepted by the human skin, and our results show ingrowth of functional collagen-producing fibroblasts and blood vessels. The inflammation noticed was not judged to inhibit ingrowth of fibroblasts and endothelial cells and declined over time.

## Paper II

All subjects completed the investigation, and no adverse events or signs of inflammation or rejection were seen. Distinct weals were created easily with the gelatin spheres and the saline solution. The cross-linked HA seemed to diffuse more than the gelatin spheres and the saline solution and less well-defined weals were created.

After two weeks, histological examination of the controls (saline solution) demonstrated normal human skin as expected. The cross-linked HA occupied space and compressed the surrounding dermal tissue. No ingrowth of cells into the cross-linked HA could be seen, but an increase in cells, judged to be inflammatory cells, around the implants was noted. The gelatin spheres were populated by cells after two weeks with the highest density of cells within the spheres closest to normal dermis. Closest to the dermis, collagen bundles were also seen between and inside the spheres (Figure 15).

When eight weeks had passed, the saline solution and the crossed-linked HA demonstrated the same picture as after two weeks except that the inflammatory response had declined around the cross-linked HA. The gelatin spheres were completely occupied by cells, and structures interpreted as blood vessels could be seen. The spheres had collapsed partly because of degradation and were substituted by newly formed connective tissue.

The histological examination at the next time point, 12 weeks, showed that the crossed-linked HA still occupied some space, but it had decreased in amount due to degradation. The gelatin spheres demonstrated continued degradation and replacement by dermal tissue. Visually the new dermal tissue had the same

appearance as the original dermal tissue as a sign of regeneration instead of scar formation.

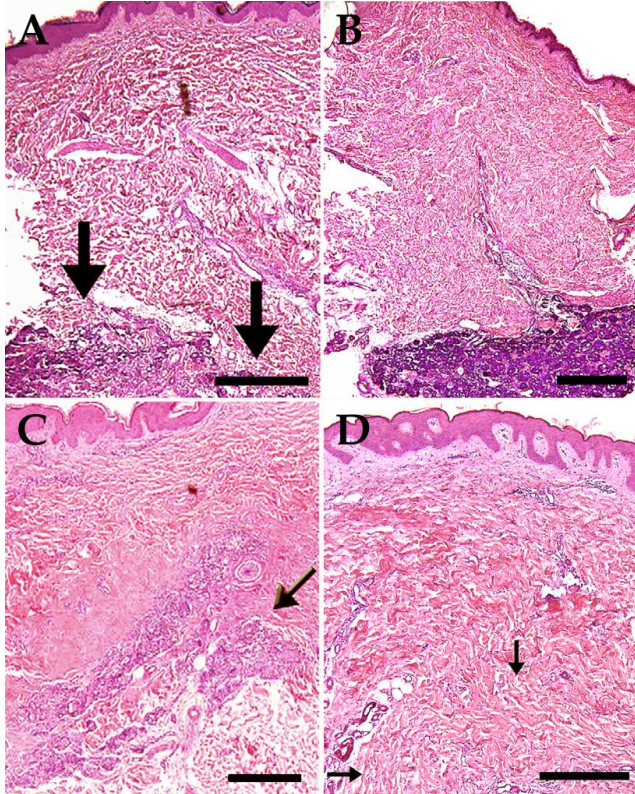


**Figure 15.** Hematoxylin and eosin staining of injected gelatin spheres. (A) Histological picture two weeks after injection. The weal formation of the overlying tissue is still present. (B) Eight weeks after injection. The gelatin spheres are completely occupied by fibroblasts and connective tissue. A close-up view shows increased internal pore size as a sign of degradation (not shown in this picture). (C) Twelve weeks after injection, the gelatin spheres have further degraded, and newly formed connective tissue is seen. (D) Twenty-six weeks after injection, only small remnants of the gelatin spheres are visible, and the newly formed dermis seems to have normal architecture. Arrows indicate sites of injections (bars = 500  $\mu\text{m}$ ).

At the final time point, 26 weeks, only a small amount of cross-linked HA could be detected. The gelatin spheres had undergone further degradation and could only be localized as small remnants. The space between the remnants was completely filled with vascularized regenerated dermal tissue.

Vascularization of the regenerated dermis within the gelatin spheres was confirmed by immunohistochemical staining with monoclonal mouse-antihuman von Willebrand factor antibody (Figure 16). The staining pattern was of tubular structures going deep into the newly formed dermis, and red blood cells were present within the lumens. No neo-angiogenesis could be seen within the cross-linked HA.

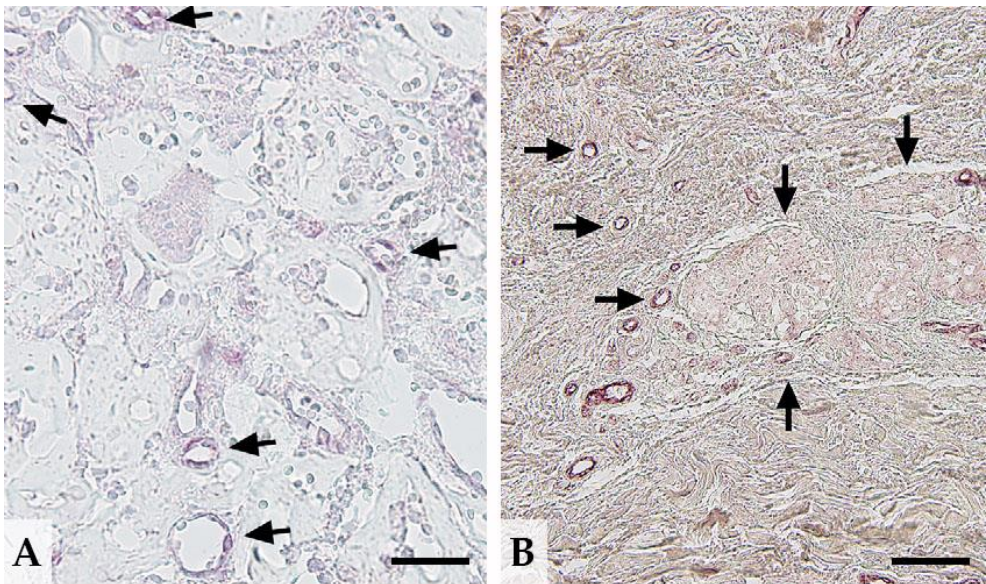


**Figure 16.** Immunohistochemical staining for von Willebrand factor of injected gelatin spheres after (A) two weeks and (B) eight weeks. Arrows indicate positive staining for endothelial cells in the blood vessel walls within the injected scaffold (bars = 50  $\mu\text{m}$  in A and 100  $\mu\text{m}$  in B).

The biodegradable gelatin sphere was initially developed for high-density *in vitro* cell culture [104]. Gelatin is a degradation product of collagen and is further degraded without any toxic waste products. Earlier studies within the research group have shown that the porous gelatin spheres are a suitable matrix for guided tissue regeneration [114, 115]. They can be used as a liquid and injectable three-dimensional scaffold. We consider the gelatin spheres to be easy to prepare and inject in dermis. They seem to be suitable as a template for dermal regeneration.

## Paper III

A culture media containing 50% amniotic fluid (AF), significantly accelerates ( $p < 0.05$ ) the healing of human cutaneous skin wounds *in vitro* when compared to the healing of identical wounds cultured in ordinary culture media. After three days of incubation in 50% AF, the wounds were re-epithelialized by 33%. After seven days, they were almost completely re-epithelialized (94% re-epithelialization). For wounds incubated in 10% FCS (ordinary culture media used as control), 43% of the wound surface was re-epithelialized after three days and 52% after seven days (Figure 18). Previous studies using the same *in vitro* skin wound model have shown that AF can induce wound healing down to a concentration of 25% without adding serum [116].

DMEM was chosen as negative control, and no re-epithelialization was seen at any time point, as expected. A concentration of 10% AF was not sufficient to induce re-epithelialization. The group incubated in 50% FCS was chosen to get an excess of nutrients, but no significant differences could be shown between this group and 50% AF.

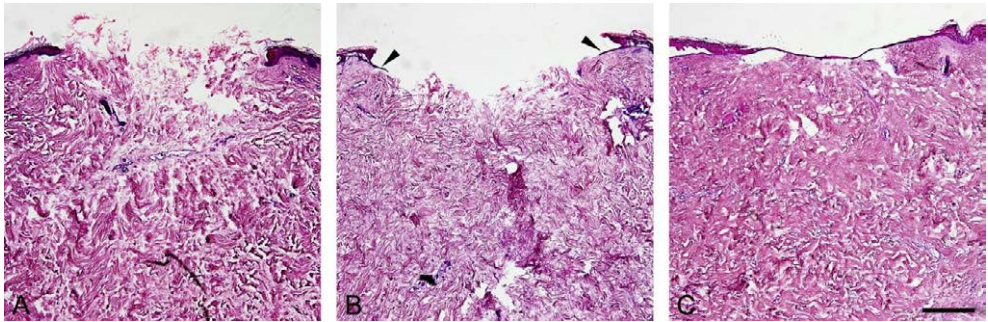


**Figure 17.** Hematoxylin and eosin staining of wounds show different grades of re-epithelialization. (A) No re-epithelialization in a sample incubated in 10% AF for three days. (B) A partially re-epithelialized wound (arrowheads show epidermal tongues at the wound margins) after incubation in 10% FCS for seven days. (C) Complete re-epithelialization of a wound after seven days of incubation in 50% AF (bar = 1000  $\mu$ m).

10 % AF: 90% Dulbecco's modified Eagle's medium and 10% amniotic fluid; 10% FCS: 90% Dulbecco's modified Eagle's medium and 10% fetal calf serum; 50% AF: 50% Dulbecco's modified Eagle's medium and 50% amniotic fluid.

Degradation of HA in 50% AF by adding hyaluronidase significantly decreased ( $p < 0.05$ ) the ability of AF to induce re-epithelialization. Only 8% and 25% of the wound surface was re-epithelialized in wounds incubated in 50% AF with degraded HA after three and seven days respectively, which was significantly lower ( $p < 0.05$ ) than in wounds incubated in 50% AF. After 12 days, 98% of the wound surface was re-epithelialized in wounds incubated in 50% AF with degraded HA, and there was no longer a significant difference.

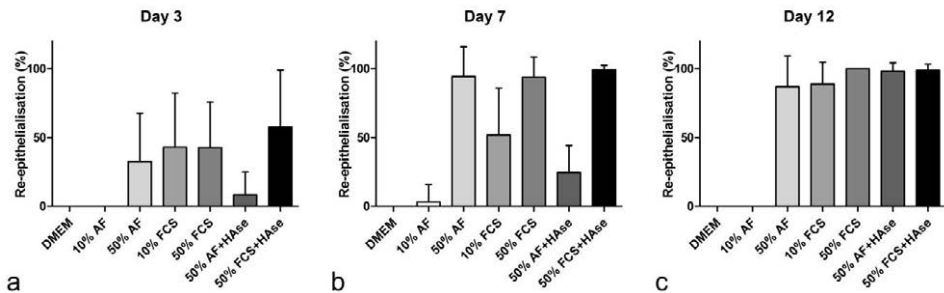


**Figure 18.** Figure showing re-epithelialization of human skin wounds *in vitro* after incubation for three, seven, and twelve days. Fifty percent AF displayed a significantly higher grade of re-epithelialization ( $p < 0.05$ ) as compared to DMEM as well as 10% AF at all time points and showed significantly higher ( $p < 0.05$ ) grade of re-epithelialization compared to 10% FCS at seven days. Degradation of hyaluronic acid in 50% AF significantly impaired the re-epithelialization at day three and seven ( $p < 0.05$ ).

DMEM: 100% Dulbecco's modified Eagle's medium; 10% AF: 90% Dulbecco's modified Eagle's medium and 10% amniotic fluid; 50% AF: 50% Dulbecco's modified Eagle's medium and 50% amniotic fluid; 10% FCS: 90% Dulbecco's modified Eagle's medium and 10% fetal calf serum; 50% FCS: 50% Dulbecco's modified Eagle's medium and 50% fetal calf serum; 50% AF + HAse: 50% Dulbecco's modified Eagle's medium and 50% amniotic fluid + hyaluronidase; 50% FCS + HAse: 50% Dulbecco's modified Eagle's medium and 50% fetal calf serum + hyaluronidase.

The addition of hyaluronidase affected the wound-healing properties of AF but not those of FCS. Our results indicate that HA is an important factor for the wound-healing properties of AF. Re-epithelialization was measured at three, seven, and twelve days to study the entire process of re-epithelialization.

Twelve days was chosen as a final time point as a wound normally heals within two to twelve days [16]. FCS at a concentration of 10% was used as positive control, and healing time could be compared to that in a normal wound healing milieu.

The number of skin donors on the same day was restricted, and the amount of skin from each donor was also limited. The groups in this study are therefore small, and skin from only three donors is used. Repeated experiments with the same experimental set-up would enable larger groups and strengthen the results.

The concentration of hyaluronidase in this experiment is more than 1000-fold higher than that measured in fetal wound fluid [78]. AF has HA-stimulating activity and might stimulate the fibroblasts to produce HA to some extent [117]. AF might also inhibit hyaluronidase [60], but researchers have not investigated whether this is applicable to hyaluronidase from the *Streptomyces hyalurolyticus* that was used in this study. The considerable difference in re-epithelialization between seven and twelve days of incubation in AF with added hyaluronidase compared to AF without hyaluronidase could possibly be loss of enzymatic activity or production of HA, but we hypothesize that the re-epithelialization is only delayed due to the degradation of HA and occurs later.

In conclusion, AF promotes accelerated re-epithelialization in human adult *in vitro* skin wounds, and HA is an important factor in this process.

## Paper IV

All 10 subjects completed the investigation, and no adverse events or unexpected skin reactions were noted. The laboratory results were within reference ranges both at the beginning and the end of the study except for one subject that had a prolonged activated partial thromboplastin time (APTT). This subject was excluded from further analysis with proteomics and is not included in analysis of TiVi data or the

statistical calculations of histological evaluation. The earlier described minimally invasive wound model was successfully further developed to the present settings.

The wounds and biopsy specimens were intended to be as small as possible to minimize scarring (Figure 22) but still be of a size that could be handled for histology and that contained enough protein for analysis.

The most pronounced erythema was seen 24 hours after incisions in all subjects (Figure 19). It then subsided over time and had returned close to baseline levels after 14 days. The results, when we used TiVi instead of laser Doppler-based technologies, are in concordance with earlier studies [102]. However, no inflammatory response could be detected between the interventions, suggesting that exogenous intradermal HA does not affect the inflammatory response as measured by TiVi. The half-life of HA is short in skin [118], and high molecular weight HA and its shorter break-down products have different biological effects. Generally, high molecular weight HA is thought to decrease inflammation while the shorter break-down products are pro-inflammatory [79, 119, 120]. At 24 hours, the many cells observed in the wounds histologically were believed to be inflammatory; however no immunohistological evaluation was conducted to confirm this notice, and no quantification between the groups has been done.

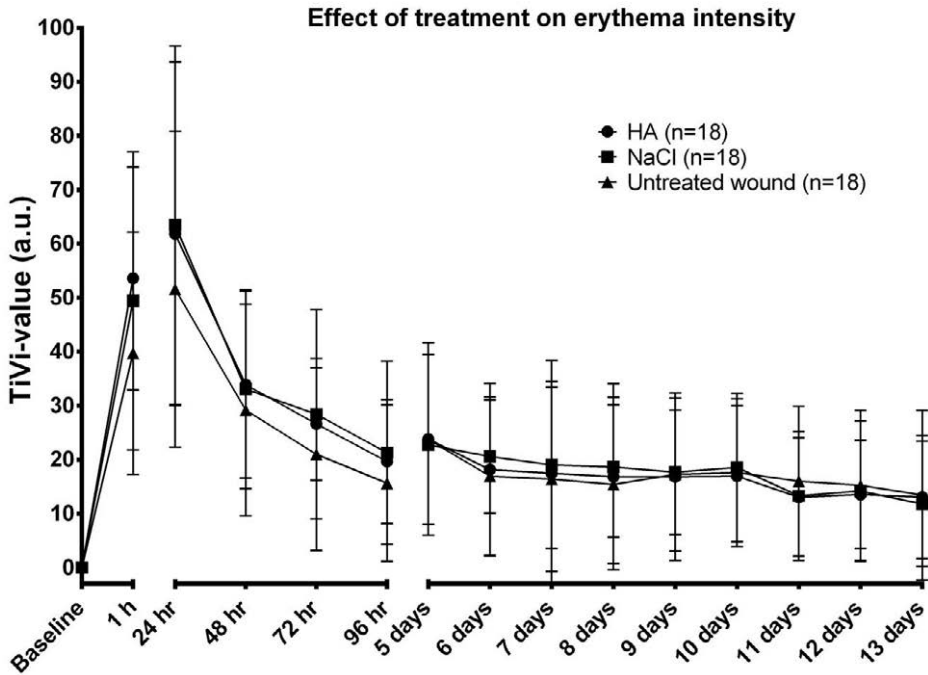


**Figure 19.** Results from tissue viability imaging (TiVi). Wounds injected with hyaluronic acid (HA) or saline solution (NaCl) and untreated wounds at a group level ( $n=18$ ) are shown as mean TiVi-values (erythema intensity). No difference in the erythema intensity between the treatments could be detected using the TiVi system. Data were normalized by the subtraction of baseline (TiVi values for unprovoked skin). Error bars show  $\pm 1$  SD.

The wounds were found to be easily detectable when using standard procedure for cutting cross sections and staining (Figure 20). Nevertheless, two wounds could not be identified in the biopsies. These biopsies were two of the first to be embedded in paraffin, and the lack of wounded tissue was probably due to erroneous orientation of the skin specimens.

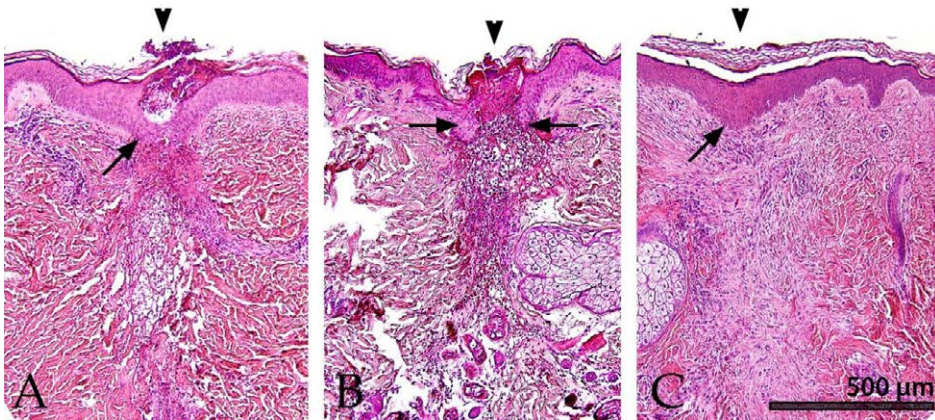


**Figure 20.** Hematoxylin and eosin staining of biopsies demonstrating different grades of re-epithelialization. (A) Healed epidermis and partial reformation of the cornified envelope was seen in the group treated with hyaluronic acid already after 24 hours. (B) In contrast, wounds treated with saline solution (9 mg/ml) showed incomplete healing after 24 hours. (C) After 14 days, all wounds in all groups were re-epithelialized and completely cornified. Picture showing wound treated with sodium chloride after 14 days. Arrowheads indicate wound sites and wound directions, while the arrows indicate the epidermis.

All wounds were found to be deep dermal and of the same size. Six of seven wounds in the HA group were completely re-epithelialized after 24 hours of wound healing; in contrast, no wounds were re-epithelialized in the saline solution group, and two were re-epithelialized in the control wounds with no injection prior to wounding (Table 6). Wounds treated with HA demonstrated significantly ( $p < 0.05$ ) faster re-epithelialization than wounds treated with saline solution. No significant difference could be proven between wounds treated with HA compared to untreated wounds. The results from our study support the hypothesis that HA stimulates migration and proliferation of keratinocytes, and we saw these differences even if the HA was exogenous.

Subject	HA	NaCl	Untreated wound
1*	1	0	-
2*	1	0	-
3	1	0	0
4	1	0	1
5	1	0	0
6	1	0	0
7*	1	0	1
8	1	0	1
9	1	0	0
10	0	0	0

**Table 6.** Results from histological evaluation of the re-epithelialization at 24 hours. Total re-epithelialization was scored “1,” and less than 100 percent re-epithelialization was scored “0.” Subjects marked with asterisks were excluded from statistical calculations.

The focus of this study was histologically on the epidermal part of the wound-healing process. However, we morphologically studied the dermal tissue. At 24 hours, many cells judged to be red blood cells and inflammatory cells were noted in the dermal wounds. After 14 days, there were considerably fewer cells at visual inspection. The cells tended to be in the middle of the prior wound, and newly formed dermal tissue with densely packed fibers was seen. The dermal scar was well-visible after 14 days in all groups. In future studies, we aim to more closely investigate dermal wound healing and scar formation.

We found the protein concentration in a 2-mm skin biopsy to be sufficient for proteomic analyses. Altogether, 168 spots were matched in all eight gels and

included for spot quantification (Figure 21). Pooling the protein from nine subjects resulted in comparisons at group levels, which we were interested in, but pooling also decreased the possibility of performing statistical analyses. Using the 2-DE electrophoresis with protein identification by mass spectrometry provides a high specificity for the detected proteins and allows isoforms of proteins to be detected as well.

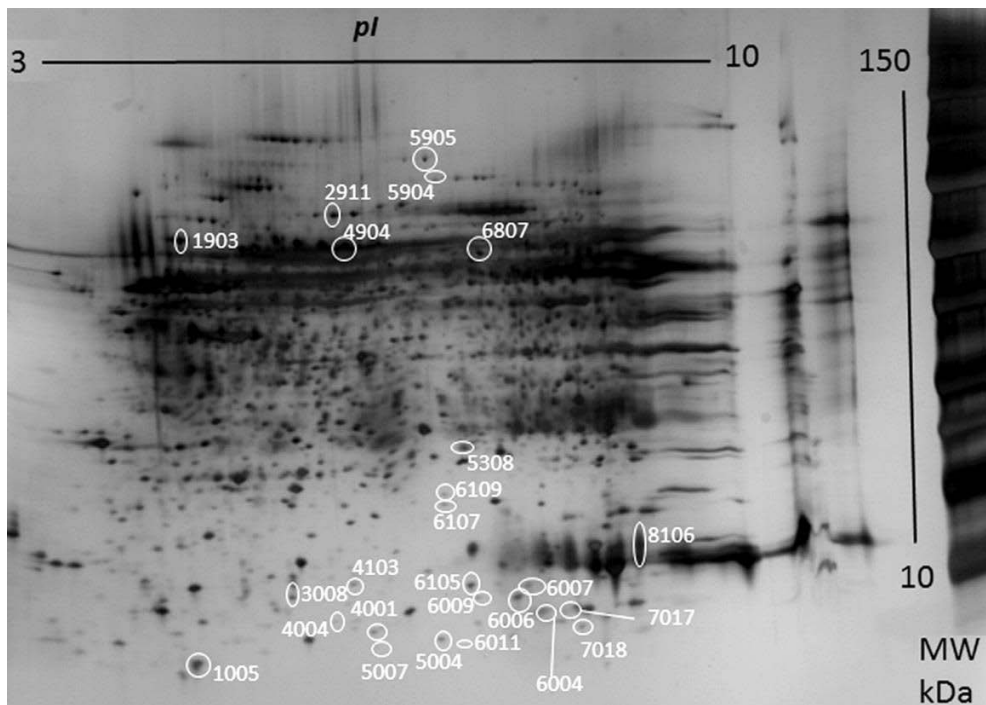


**Figure 21.** A two-dimensional electrophoresis gel with the protein pattern of human skin from pooled samples. Spots were recognized, numbered, and compared using PDQuest software. Several spots were further identified by mass spectrometry.

Based on protein patterns in the 2-DE from pooled samples, we analyzed the data using a multivariate projection model, the orthogonal partial least squares regression (OPLS) with discriminant analysis (DA). Both presented models resulted in (non-

significant) over-fitted OPLS-DA (Figure 23). Analyzing the proteomic data with multivariate projection detects relationships or differences between the groups; HA1 and HA13 seemed to be separated from both untreated wound1/13 and NaCl1/13 as well as from each other. As the data used in the statistical analyses came from pooled samples, there is no measure of intra-group variation. The multivariate approach can show us trends in the datasets that approximate group similarities, but we must use the results of such analyses carefully and conservatively. Expanding the data by running gels for each sample per group would provide more power in the statistical treatment of data, and our conclusions might be modified in accordance with such findings.

Of the 14 proteins detected to be at least 10-fold changed between HA1 and untreated wound1, 11 have been identified: eight as up-regulated and three as down-regulated. Out of the eight proteins detected to be at least 10-fold changed between HA1 and NaCl1, three have been identified so far (Table 7). Two of the identified proteins, were found regulated at least 10-fold in both groups and these were Fibrinogen beta chain and Protein S100-A8.

Fibrinogen beta chain was found to be down-regulated in wounds injected with HA compared to both untreated wounds and wounds injected with saline solution at 24 hours. Fibrinogen beta chain is a fibrinogen subunit belonging to the acute phase proteins, and the concentration normally increases during inflammation [121]. Fibrinogen is a principal factor in the maintenance of hemostasis. It is mainly produced by the liver but is also produced extrahepatically during inflammation, playing a role in localized injury and repair [122].

Protein S100-A8 was found up-regulated in wounds after injection with HA compared to injection with saline solution or untreated wounds. This member of the S100 protein family is a calcium-binding protein involved in inflammation, innate

immunity, tissue damage, wound healing, stress response, cell motility, proliferation, and differentiation [123] as well as regulating tumor cell proliferation [124]. S100-A8 is mainly expressed in granulocytes and epithelial cells [125] and has been shown to be especially involved in facilitating the growth of new vessels during inflammation [126]. Further on, S100-A8 is found enriched in wound fluid from diabetic wounds at day two of wound healing [127]. Its role is suspected to be the differentiation of fibroblasts and accumulation of monocytes in areas of inflammation [128, 129].

Pre-treatment with exogenous HA does not affect the inflammatory process during deep dermal wound healing, as measured by TiVi. The histological results show that injection of HA prior to the incision has a positive effect on re-epithelialization. Wounds treated with exogenous HA also show altered protein expression compared to wounds treated with saline solution or untreated wounds. These results from our present study are in concordance with previous findings, and they suggest that exogenously HA administered intradermally has a positive effect on the healing process of deep dermal wounds.

We conclude that exogenous intradermal HA accelerates re-epithelialization and alters protein expression in human *in vivo* deep dermal skin wounds. These results indicate that HA might be an important component in future regimes aiming at an improved wound-healing process.

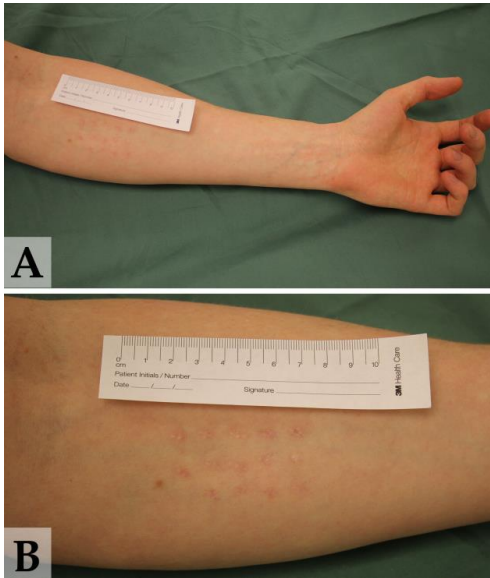


**Figure 22.** Photograph of study area in a subject one year after the study. Only small scars are visible.

Photograph published with permission from the subject.

Spot ID	UniProt	Protein name	Sequence coverage %	Untreated wound1 vs. untreated wound13	HA1 vs. NaCl1	HA1 vs. untreated wound1	HA13 vs. NaCl13	HA13 vs. untreated wound13
0004	P25815	Protein S100-P	30.5	↓	-	↓	↑	↑
1005	P06703	Protein S100-A6	25.9	↑	-	-	-	-
1903	P01009	Alpha1-antitrypsin	56	-	-	-	-	↑
4001	P31151	Protein S100-A7 (Psoriasis)	21.8	-	-	↑	-	↑
4004	P26447	Protein S100-A4	27.7	-	-	↑	-	↑
4904	P02768	Serum albumin	17.7	-	-	↓	↑	-
5004	P47929	Galectin-7	71	↑	-	-	-	-
5308	P60174	Triosephosphate isomerase	38.5	-	-	-	-	↑
6004	P05109	Protein S100-A8	39.8	-	-	↑	↑	↑
6006	P05109	Protein S100-A8	48.4	-	-	-	-	↑
6007	P05109	Protein S100-A8	48.4	-	-	-	↑	↑
6009	P60903	Protein S100-A10 (Calpactin I light chain)	45.4	-	-	-	↑	↑
6105	Q9NZT1	Calmodulin-like protein 5	8.9	-	-	↑	-	-
6107	P62937	Peptidyl-prolyl cis-trans isomerase A	35.2	-	-	-	-	↑
6109	P23528	Cofilin-1	79.5	-	-	-	-	↑
6807	P02675	Fibrinogen beta chain	62.9	-	↓	↓	-	-
7017	P05109	Protein S100-A8	32.3	-	↑	↑	-	↑
7018	P81605	Dermcidin; Survival-promoting peptide	20	-	-	↑	-	↑
8106	P69905	Hemoglobin subunit alpha	77.5	-	-	-	-	↓
0002	Q9NZT1	Calmodulin-like skin protein	8.9	↑	-	↑	↑	-
2911	P06396	Gelsolin	39.6					
5904	P02787	Serotransferrin	20.3					
5905	P15924	Desmoplakin	5.2	↑	↑	-	-	-
3008	P06702	Protein S100-A9	81.6	↑	-	-	-	-
4103	P06702	Protein S100-A9	81.6	↑	-	↑	-	↑

Table 7. List of identified proteins that were at least 10-fold altered.

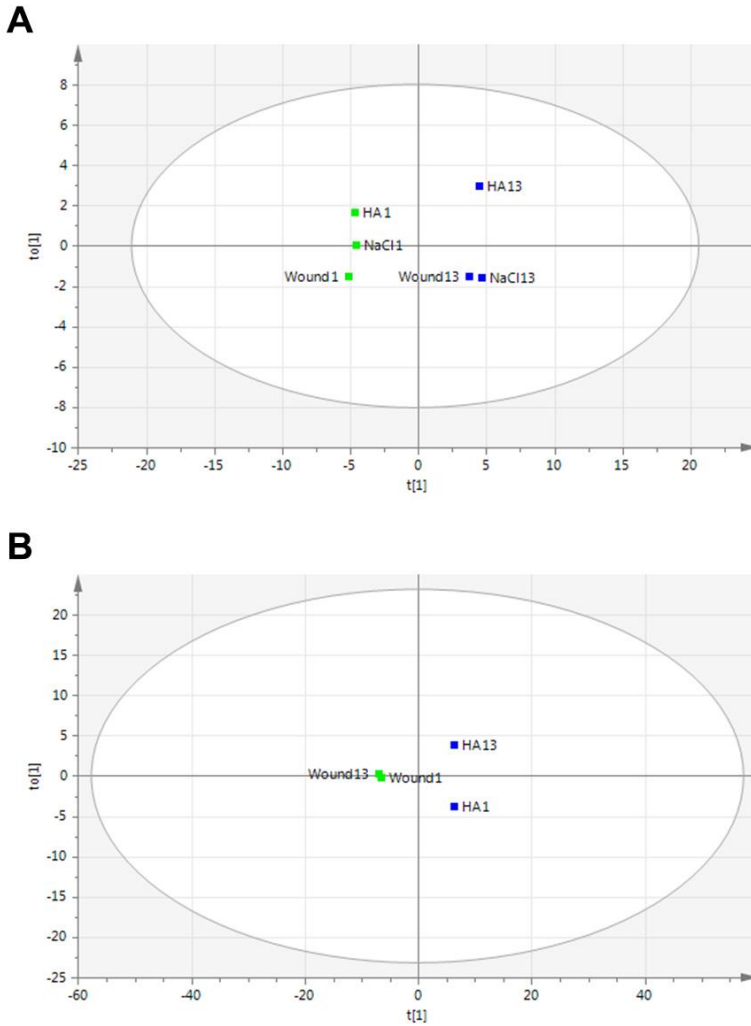


**Figure 23.** Multivariate projection models. (A) This model included the following groups: untreated wounds day 1 (wound1), untreated wounds day 13 (wound13), saline-treated wounds day 1 (NaCl1), saline-treated wounds day 13 (NaCl13), hyaluronic acid-treated wounds day 1 (HA1), and hyaluronic acid-treated wounds day 13 (HA13). Clustering indicated differences accountable by time. (B) Model of groups: untreated wounds day 1(wound1), untreated wounds day 13 (wound13), hyaluronic acid-treated wounds day 1 (HA1), and hyaluronic acid-treated wounds day 13 (HA13) show a clustering trend that differs between treatments. Data are not significant.

# Concluding Remarks and Future Perspectives

In Papers I and II, we studied whether dermal scarring could be turned into regeneration by using two different types of three-dimensional dermal scaffolds. Both materials showed ingrowth of functional fibroblasts and blood vessels and seemed to stimulate regeneration while slowly degrading. This could be of significant clinical importance, for example in burn wound care or after cancer surgery.

Both scaffolds studied in this thesis show properties of functioning as a matrix for guided regeneration of the dermis. However, the gelatin spheres are most in focus for further studies. We are interested in studying the clinical application of the gelatin spheres, for example using them for soft tissue deficit after breast cancer surgery instead of fat transplantation or for improving the visual appearance of scar tissue.

In Paper III and IV, we wanted to study the effects of amniotic fluid (AF) and hyaluronic acid (HA) on adult wound healing as early fetal wounds re-epithelialize fast and naturally heal dermis without scarring but by regeneration and without the need for dermal substitutes. We found that AF had a positive effect on adult wound healing *in vitro*, and our findings support the importance of HA in this process.

Stimulation with exogenous HA *in vivo* induced accelerated re-epithelialization and an altered protein expression.

Elucidating the effects of AF on wound healing and the role of HA may allow improved treatment of wounds with impaired healing. The complex composition of AF gives rise to the question of other factors, potentially positive to wound healing, that still need to be investigated. Further studies, that analyze the gene expression in fibroblasts and keratinocytes, while cultured in AF may also contribute to the detection and isolation of key molecular events related to the healing process.

We conclude that the earlier described minimally invasive human *in vivo* wound model functions well when further developed to be combined with tissue viability imaging, histology, and proteomics. We believe that the model has many applications and can be of great value for further studies of wound healing with different set-ups and interventions. In the present study, our focus was on epidermal regeneration. We are certainly interested in future analyses regarding dermal wound healing. Additional studies of the dermal tissue, for example, might include examination of the differences in the number of inflammatory cells, collagen deposition, and the presence of myofibroblasts. To supplement the proteomic results, immunohistochemistry could provide stronger evidence for the presence of selected proteins. We are also interested in looking at non-pooled data to see differences between individuals, both after the influence of HA and during the normal wound-healing process. Interesting proteins identified in the present material can be further studied using the *in vitro* wound model used in Paper III.

Although the wound-healing process is a well-studied field, much knowledge must be gained to unlock the door to the regenerative pathway in humans. Studies on finding new dermal substitutes and studies on the positive effect of AF and HA on

wound-healing process are two different ways of gaining insight that may lead to improved wound healing for the patient.



# Populärvetenskaplig sammanfattning

## Popular Scientific Summary in Swedish

Varje dag och överallt i världen får människor skador på sin hud som en del av sin vardag. Sår av alla de slag och storlekar uppstår och en del passerar individen obemärkt. För kroppen är huden mycket viktig som ett yttre skydd, och då även en liten sårskada innebär att hudens viktiga barriärfunktion blir äventyrad, svarar kroppen direkt med att sätta igång den vardagliga men samtidigt mycket komplicerade processen som kallas sårsläkning. Större akuta sår och kroniska sår leder ofta patienten till sjukvården. Sår leder allt för ofta till mycket lidande för den enskilde individen och innebär samtidigt även stora kostnader för samhället. Omfattande brännskador intar i sammanhanget en särställning med dess livshotande initiala fas och därefter långdragna läkningsförlopp med infektionsrisker och funktionsnedsättande ärrbildning.

Huden är ett av kroppens största organ med flera viktiga funktioner. Den är hos en vuxen individ cirka två kvadratmeter stor och varierar i tjocklek utifrån lokalisation på kroppen. Det yttre lagret av huden kallas överhuden. Överhuden utgör skyddet mot omgivningen och består av flera lager celler. Under överhuden återfinns

läderhuden bestående av celler och bindväv. Läderhudens har till uppgift att ge elasticitet och styrka till huden men här återfinns även hårkörtlar, svettkörtlar och känselorgan. Utöver ovan nämnda barriärfunktion så har huden bland annat även till uppgift att förmedla beröring och smärta, reglera temperatur samt att tillverka D-vitamin.

Överhuden nybildas konstant och läker med något som kallas regeneration, vilket innebär att ny hud med samma utseende som den före skadan återskapas efter ett sår. Om sårskadan går djupare i huden och går ner till den underliggande läderhuden finns inte samma möjlighet till perfekt läkning. Läderhuden läker med ärrbildning och inte med regeneration. Vid små sårskador kan detta ärr inte ses med blotta ögat. Efter skada och ärrbildning av läderhuden kan den bli mycket tunn, torr och oelastisk samt sakna hår och känsel.

Sår-läkningsprocessen är välstuderad men mycket återstår att lära innan vi kan återskapa hud snabbt och utan ärrbildning. Den här avhandlingen syftar till att studera olika aspekter av sår-läkningsprocessen med ett fokus på om vi kan styra överhudens regeneration samt stimulera läderhuden till regeneration. Ett sätt att försöka få läderhuden att regenerera är att tillföra ett tredimensionellt matrix, ett material hudens celler kan växa in i och bryta ner, emedan ny hud återskapas.

I de två första arbetena har vi studerat två tredimensionella matrix för att försöka stimulera läderhuden att regenerera enligt ovan. I arbete I använde vi ett syntetiskt material gjort av polyuretanurea. Först studerade vi på laboratoriet om läderhudens bindvävsceller kunde växa in i materialet och sedan opererade vi in små bitar av materialet i läderhuden hos friska försökspersoner. I arbete II valdes en annan strategi där vi istället sprutade in ett flytande tredimensionellt matrix i form av porösa gelatinkulor i läderhuden på friska försökspersoner. Båda studierna visade att

bindvävsceller och kärl växte in i materialen. Matrixen bröts sakna ner och ersattes med ny hud på ett sätt som liknade regeneration.

Under de första två tredjedelarna av fostertiden har det mänskliga fostret en förmåga att läka hela huden snabbt och utan ärrbildning. Om vi kunde få huden hos människan att reagera på ett liknande sätt även efter födseln, som under den tidiga fostertiden, skulle metoderna med matrix som beskrevs ovan inte behövas. Människans gener ändras inte efter födseln och det har föreslagits att fostermiljön är inblandad i varför fostret läker utan ärr. Fostrets hud omges av varmt, sterilt fostervatten som bland annat innehåller många näringsämnen, tillväxtfaktorer och ett ämne som heter hyaluronsyra. Hudens bindväv består till stor del av just hyaluronsyra.

I arbete III och IV har vi velat studera om vi kan påverka människans sårhäkning efter födseln genom att tillföra fostervatten eller hyaluronsyra och på så sätt styra sårhäkningen så att den mer liknar fostrets sårhäkning. I arbete III "odlade" vi på laboratoriet överbliven hud från plastikkirurgioperationer i olika näringslösningar där bland annat fostervatten ingick. Vi tillverkade standardiserade sår i huden och såg att de läkte snabbt när huden odlades i fostervatten. När vi avsiktligt tillförde ett enzym som bryter ner hyaluronsyra försämrades till viss del fostervattnets gynnsamma effekt på sårhäkningen.

I arbete IV ville vi fortsättningsvis studera hyaluronsyrans effekt på sårhäkning hos friska försökspersoner. Vi sprutade in hyaluronsyra i läderhuden och skapade därefter små sår i huden med hjälp av lansetter för blodprovstagning (samma som används för "stick i fingret"). Vi fann att såren som behandlats med hyaluronsyra läkte snabbare än om de behandlats med koksalt samt att det var skillnad i vilka proteiner som bildades av huden. Vi mätte även rodnaden kring såren, som ett mått

på inflammation, genom att fotografera med polariserat ljus men vi kunde inte uppmäta någon skillnad mellan grupperna med den tekniken.

Forskning om sårhäkning, till exempel utveckling av nya matrix för att stimulera regeneration eller studier av fostervatten och dess beståndsdelars positiva effekt på sårhäkning, är två potentiella vägar att nå kunskap som på sikt leder till att sårhäkning kan styras mot snabb regeneration. Påskyndad sårhäkning med minimal ärrbildning skulle i många sammanhang vara önskvärd och, när det gäller svåra sår, vara helt avgörande för överlevnad, minskat lidande, god funktion och behov av sjukvård.

# Acknowledgements

I would like to express my gratitude to all the people who have contributed to making this thesis possible. Especially I would like to acknowledge:

**Gunnar Kratz**, for being my brilliant supervisor throughout this whole process; always positive, inspiring and full of good ideas. I cannot thank you enough!

**Fredrik Huss**, co-supervisor and co-author, for introducing me into the world of research when I was a third year medical student. Thank you for giving me the chance to start this project.

**Kristina Briheim** and **Anita Lönn**, senior lab technicians, for teaching me cell culture and good laboratory practice.

**Johan Junker**, laboratory colleague and co-author, for being a practical supervisor at the lab and helping me out with the third paper when I needed a push in the right direction. I hope you come back here someday.

**Joakim Henricson**, co-supervisor and co-author, for teaching me about TiVi, being such a helpful and positive person, and cheering me up when I needed it the most. "There are oceans of time."

**Jonathan**, co-worker at the lab and co-author, for, help, criticism and proofreading. You are going to go far in your academic work.

**Camilla** and **Susanna**, former and present co-workers at the lab, for co-operation and making the lab a good place to work.

**Chris Anderson**, special adviser at my "half-time" and co-writer of the fourth paper, for introducing the minimal invasive wound model that made my thesis take the last interesting turn.

**Bijar Ghafouri**, co-author of the fourth paper, for guiding me through the jungle of proteins.

All subjects and donors that have contributed in the different studies. For the “healthy males below forty” that volunteered in the fourth paper; as promised, you will be invited for Champagne when the paper is published.

**Göran Nylander**, my former head at the Hand- and Plastic Surgery Department, for giving me the opportunity to have one of the best jobs in the world and for all the pushing, guidance and teaching. I am so glad that I did this.

**Thomas Hansson**, my present chief at the Hand- and Plastic Surgery Department, for friendship, leadership, support and for sharing your hand surgery skills with me. Now I am coming back to the clinic even if I plan to continue with my academic adventures.

**Ulf Larsson** for being my first practical tutor and assisting me hundreds of times when I took my first tentative steps toward becoming a hand surgeon.

**Carin Rubensson**, roommate, colleague and friend, for sharing good ideas, laughs and secret drawers.

**Johan Thorfinn** for being my unauthorized mentor.

Colleagues at the Hand- and Plastic Surgery Department, **Magnus Berggren**, **Lars-Erik Karlander**, **Simon Farnebo**, **Max Bergkvist** and **Maria Moloney** as well as all the plastic surgeons, for friendship, cooperation and covering for me when I was out of duty.

**My friends**, some come, some go and some stay through my whole life. I do not need to mention your names. You know who you are.

My parents, **Birgitta** and **Lasse Svensson**, for loving and raising me. You have always supported me in all kinds of ways and have been the best parents I could wish for.

**Ingrid** and **Tonny Nyman**, my parents-in-law, for taking me into your family as your own daughter.

My brothers and sister; **Klas**, **Per**, and **Kristina**, for giving me a big family to grow up with and being such important persons in my life. Without you, nothing would be the same.

My brothers-in-law, **Per** and **Henrik**, you are like real brothers to me.

My wonderful and beloved three children, **Elvin**, **Anton** and **Mira**, for giving my life true meaning.

**Tobbe**, the love of my life and my best friend in the world, for your love, friendship, academic discussion and 24/7 IT-support. You have already been there half of my life, but there is more to come. I hope we will continue to fill “our storybook of love.”



# References

1. Sen, C.K., et al., *Human skin wounds: a major and snowballing threat to public health and the economy*. Wound Repair Regen, 2009. **17**(6): p. 763-71.
2. Wood, L.C., et al., *Barrier disruption stimulates interleukin-1 alpha expression and release from a pre-formed pool in murine epidermis*. J Invest Dermatol, 1996. **106**(3): p. 397-403.
3. Coulombe, P.A., *Towards a molecular definition of keratinocyte activation after acute injury to stratified epithelia*. Biochem Biophys Res Commun, 1997. **236**(2): p. 231-8.
4. Barrientos, S., et al., *Growth factors and cytokines in wound healing*. Wound Repair Regen, 2008. **16**(5): p. 585-601.
5. Pastar, I., et al., *Epithelialization in Wound Healing: A Comprehensive Review*. Adv Wound Care (New Rochelle), 2014. **3**(7): p. 445-64.
6. Watt, F.M., C. Lo Celso, and V. Silva-Vargas, *Epidermal stem cells: an update*. Curr Opin Genet Dev, 2006. **16**(5): p. 518-24.
7. Plikus, M.V., et al., *Epithelial stem cells and implications for wound repair*. Semin Cell Dev Biol, 2012. **23**(9): p. 946-53.
8. Lu, C.P., et al., *Identification of stem cell populations in sweat glands and ducts reveals roles in homeostasis and wound repair*. Cell, 2012. **150**(1): p. 136-50.
9. Eckert, R.L., *Structure, function, and differentiation of the keratinocyte*. Physiol Rev, 1989. **69**(4): p. 1316-46.
10. Singer, A.J. and R.A. Clark, *Cutaneous wound healing*. N Engl J Med, 1999. **341**(10): p. 738-46.
11. Gabbiani, G., G.B. Ryan, and G. Majne, *Presence of modified fibroblasts in granulation tissue and their possible role in wound contraction*. Experientia, 1971. **27**(5): p. 549-50.
12. Martin, P., *Wound healing--aiming for perfect skin regeneration*. Science, 1997. **276**(5309): p. 75-81.
13. Darby, I.A., et al., *Fibroblasts and myofibroblasts in wound healing*. Clin Cosmet Investig Dermatol, 2014. **7**: p. 301-11.
14. Merkel, J.R., et al., *Type I and type III collagen content of healing wounds in fetal and adult rats*. Proc Soc Exp Biol Med, 1988. **187**(4): p. 493-7.

15. Bluff, J.E., et al., *Bone marrow-derived endothelial progenitor cells do not contribute significantly to new vessels during incisional wound healing*. *Exp Hematol*, 2007. **35**(3): p. 500-6.
16. Gurtner, G.C., et al., *Wound repair and regeneration*. *Nature*, 2008. **453**(7193): p. 314-21.
17. Yamauchi, M., et al., *Cross-linking and new bone collagen synthesis in immobilized and recovering primate osteoporosis*. *Bone*, 1988. **9**(6): p. 415-8.
18. Moali, C. and D.J. Hulmes, *Extracellular and cell surface proteases in wound healing: new players are still emerging*. *Eur J Dermatol*, 2009. **19**(6): p. 552-64.
19. Xue, M., N.T. Le, and C.J. Jackson, *Targeting matrix metalloproteases to improve cutaneous wound healing*. *Expert Opin Ther Targets*, 2006. **10**(1): p. 143-55.
20. *Advanced Burn Life Support Course*. 2005, Chicago: American Burn Association.
21. Sjöberg, F. and L. Östrup, *Brännskador*. 2002, Stockholm: Liber AB.
22. Shier, D., J. Butler, and R. Lewis, *Hole's anatomy and physiology, 8<sup>th</sup> edition*. 1999: McGraw hill.
23. Tortora, G. and S. Grabowski, *Principles of anatomy and physiology, 8<sup>th</sup> edition*. 1996: Harper Collins College Publishers.
24. MacNeil, S., *Progress and opportunities for tissue-engineered skin*. *Nature*, 2007. **445**(7130): p. 874-80.
25. Gallico, G.G., 3rd, et al., *Permanent coverage of large burn wounds with autologous cultured human epithelium*. *N Engl J Med*, 1984. **311**(7): p. 448-51.
26. Brem, H., et al., *Healing of elderly patients with diabetic foot ulcers, venous stasis ulcers, and pressure ulcers*. *Surg Technol Int*, 2003. **11**: p. 161-7.
27. Bergan, J.J., et al., *Chronic venous disease*. *N Engl J Med*, 2006. **355**(5): p. 488-98.
28. Stojadinovic, O., et al., *Molecular pathogenesis of chronic wounds: the role of beta-catenin and c-myc in the inhibition of epithelialization and wound healing*. *Am J Pathol*, 2005. **167**(1): p. 59-69.
29. Brem, H., et al., *Molecular markers in patients with chronic wounds to guide surgical debridement*. *Mol Med*, 2007. **13**(1-2): p. 30-9.
30. Martin, P. and J. Lewis, *Actin cables and epidermal movement in embryonic wound healing*. *Nature*, 1992. **360**(6400): p. 179-83.

31. Larson, B.J., M.T. Longaker, and H.P. Lorenz, *Scarless fetal wound healing: a basic science review*. *Plast Reconstr Surg*, 2010. **126**(4): p. 1172-80.
32. Rowlatt, U., *Intrauterine wound healing in a 20 week human fetus*. *Virchows Arch A Pathol Anat Histol*, 1979. **381**(3): p. 353-61.
33. Beanes, S.R., et al., *Confocal microscopic analysis of scarless repair in the fetal rat: defining the transition*. *Plast Reconstr Surg*, 2002. **109**(1): p. 160-70.
34. Cass, D.L., et al., *Wound size and gestational age modulate scar formation in fetal wound repair*. *J Pediatr Surg*, 1997. **32**(3): p. 411-5.
35. Longaker, M.T., et al., *Studies in fetal wound healing, VI. Second and early third trimester fetal wounds demonstrate rapid collagen deposition without scar formation*. *J Pediatr Surg*, 1990. **25**(1): p. 63-8; discussion 68-9.
36. Ihara, S., et al., *Ontogenetic transition of wound healing pattern in rat skin occurring at the fetal stage*. *Development*, 1990. **110**(3): p. 671-80.
37. Buchanan, E.P., M.T. Longaker, and H.P. Lorenz, *Fetal skin wound healing*. *Adv Clin Chem*, 2009. **48**: p. 137-61.
38. Cass, D.L., et al., *Myofibroblast persistence in fetal sheep wounds is associated with scar formation*. *J Pediatr Surg*, 1997. **32**(7): p. 1017-21; discussion 1021-2.
39. Ferguson, M.W. and S. O'Kane, *Scar-free healing: from embryonic mechanisms to adult therapeutic intervention*. *Philos Trans R Soc Lond B Biol Sci*, 2004. **359**(1445): p. 839-50.
40. Lo, D.D., et al., *Scarless fetal skin wound healing update*. *Birth Defects Res C Embryo Today*, 2012. **96**(3): p. 237-47.
41. Watt, F.M. and H. Fujiwara, *Cell-extracellular matrix interactions in normal and diseased skin*. *Cold Spring Harb Perspect Biol*, 2011. **3**(4).
42. Ho, S., H. Marcal, and L.J. Foster, *Towards scarless wound healing: a comparison of protein expression between human, adult and foetal fibroblasts*. *Biomed Res Int*, 2014. **2014**: p. 676493.
43. Kennedy, C.I., et al., *Proinflammatory cytokines differentially regulate hyaluronan synthase isoforms in fetal and adult fibroblasts*. *J Pediatr Surg*, 2000. **35**(6): p. 874-9.
44. Alaish, S.M., et al., *Biology of fetal wound healing: hyaluronate receptor expression in fetal fibroblasts*. *J Pediatr Surg*, 1994. **29**(8): p. 1040-3.
45. Chen, W.Y. and G. Abatangelo, *Functions of hyaluronan in wound repair*. *Wound Repair Regen*, 1999. **7**(2): p. 79-89.

46. Olsson, M.J. and L. Juhlin, *Melanocyte transplantation in vitiligo*. *Lancet*, 1992. **340**(8825): p. 981.
47. Brittberg, M., E. Faxen, and L. Peterson, *Carbon fiber scaffolds in the treatment of early knee osteoarthritis. A prospective 4-year followup of 37 patients*. *Clin Orthop Relat Res*, 1994. **307**: p. 155-64.
48. Clark, R.A., K. Ghosh, and M.G. Tonnesen, *Tissue engineering for cutaneous wounds*. *J Invest Dermatol*, 2007. **127**(5): p. 1018-29.
49. Cornwell, K.G., A. Landsman, and K.S. James, *Extracellular matrix biomaterials for soft tissue repair*. *Clin Podiatr Med Surg*, 2009. **26**(4): p. 507-23.
50. Metcalfe, A.D. and M.W. Ferguson, *Tissue engineering of replacement skin: the crossroads of biomaterials, wound healing, embryonic development, stem cells and regeneration*. *J R Soc Interface*, 2007. **4**(14): p. 413-37.
51. Mulder, G., K. Wallin, and M. Tenenhaus, *Regenerative materials that facilitate wound healing*. *Clin Plast Surg*, 2012. **39**(3): p. 249-67.
52. Langer, R. and J.P. Vacanti, *Tissue engineering*. *Science*, 1993. **260**(5110): p. 920-6.
53. Burke, J.F., et al., *Successful use of a physiologically acceptable artificial skin in the treatment of extensive burn injury*. *Ann Surg*, 1981. **194**(4): p. 413-28.
54. Wainwright, D.J., *Use of an acellular allograft dermal matrix (AlloDerm) in the management of full-thickness burns*. *Burns*, 1995. **21**(4): p. 243-8.
55. Ma, L., et al., *Collagen/chitosan porous scaffolds with improved biostability for skin tissue engineering*. *Biomaterials*, 2003. **24**(26): p. 4833-41.
56. van der Veen, V.C., et al., *New dermal substitutes*. *Wound Repair Regen*, 2011. **19 Suppl 1**: p. s59-65.
57. Langer, A. and W. Rogowski, *Systematic review of economic evaluations of human cell-derived wound care products for the treatment of venous leg and diabetic foot ulcers*. *BMC Health Serv Res*, 2009. **9**: p. 115.
58. Adzick, N.S. and H.P. Lorenz, *Cells, matrix, growth factors, and the surgeon. The biology of scarless fetal wound repair*. *Ann Surg*, 1994. **220**(1): p. 10-8.
59. Sancho, M.A., et al., *Effect of the environment on fetal skin wound healing*. *J Pediatr Surg*, 1997. **32**(5): p. 663-6.
60. Gao, X., L.D. Devoe, and K.S. Given, *Effects of amniotic fluid on proteases: a possible role of amniotic fluid in fetal wound healing*. *Ann Plast Surg*, 1994. **33**(2): p. 128-34; discussion 134-5.

61. Somasundaram, K. and K. Prathap, *The effect of exclusion of amniotic fluid on intra-uterine healing of skin wounds in rabbit fetuses*. J Pathol, 1971. **107**: p. 127-30.
62. Modena, A.B. and S. Fieni, *Amniotic fluid dynamics*. Acta Biomed, 2004. **75 Suppl 1**: p. 11-3.
63. Tong, X.L., et al., *Potential function of amniotic fluid in fetal development---novel insights by comparing the composition of human amniotic fluid with umbilical cord and maternal serum at mid and late gestation*. J Chin Med Assoc, 2009. **72(7)**: p. 368-73.
64. Sheridan, R.L. and C. Moreno, *Skin substitutes in burns*. Burns, 2001. **27(1)**: p. 92.
65. Ravishanker, R., A.S. Bath, and R. Roy, *"Amnion Bank"--the use of long term glycerol preserved amniotic membranes in the management of superficial and superficial partial thickness burns*. Burns, 2003. **29(4)**: p. 369-74.
66. Singh, R., et al., *Microbiological safety and clinical efficacy of radiation sterilized amniotic membranes for treatment of second-degree burns*. Burns, 2007. **33(4)**: p. 505-10.
67. Ramakrishnan, K.M. and V. Jayaraman, *Management of partial-thickness burn wounds by amniotic membrane: a cost-effective treatment in developing countries*. Burns, 1997. **23 Suppl 1**: p. S33-6.
68. Bose, B., *Burn wound dressing with human amniotic membrane*. Ann R Coll Surg Engl, 1979. **61(6)**: p. 444-7.
69. Sawhney, C.P., *Amniotic membrane as a biological dressing in the management of burns*. Burns, 1989. **15(5)**: p. 339-42.
70. Lorenz, H.P., et al., *Scarless wound repair: a human fetal skin model*. Development, 1992. **114(1)**: p. 253-9.
71. Almond, A., *Hyaluronan*. Cell Mol Life Sci, 2007. **64(13)**: p. 1591-6.
72. Toole, B.P., *Hyaluronan: from extracellular glue to pericellular cue*. Nat Rev Cancer, 2004. **4(7)**: p. 528-39.
73. Longaker, M.T., et al., *Studies in fetal wound healing. V. A prolonged presence of hyaluronic acid characterizes fetal wound fluid*. Ann Surg, 1991. **213(4)**: p. 292-6.
74. Decker, M., et al., *Hyaluronic acid-stimulating activity in sera from the bovine fetus and from breast cancer patients*. Cancer Res, 1989. **49(13)**: p. 3499-505.
75. Dahl, L., et al., *The concentration of hyaluronate in amniotic fluid*. Biochem Med, 1983. **30(3)**: p. 280-3.

76. Longaker, M.T., et al., *Studies in fetal wound healing, VII. Fetal wound healing may be modulated by hyaluronic acid stimulating activity in amniotic fluid.* J Pediatr Surg, 1990. **25**(4): p. 430-3.
77. Girish, K.S. and K. Kemparaju, *The magic glue hyaluronan and its eraser hyaluronidase: a biological overview.* Life Sci, 2007. **80**(21): p. 1921-43.
78. West, D.C., et al., *Fibrotic healing of adult and late gestation fetal wounds correlates with increased hyaluronidase activity and removal of hyaluronan.* Int J Biochem Cell Biol, 1997. **29**(1): p. 201-10.
79. Prosdocimi, M. and C. Bevilacqua, *Exogenous hyaluronic acid and wound healing: an updated vision.* Panminerva Med, 2012. **54**(2): p. 129-35.
80. Stevenson, S., et al., *Differing responses of human follicular and nonfollicular scalp cells in an in vitro wound healing assay: effects of estrogen on vascular endothelial growth factor secretion.* Wound Repair Regen, 2008. **16**(2): p. 243-53.
81. Loryman, C. and J. Mansbridge, *Inhibition of keratinocyte migration by lipopolysaccharide.* Wound Repair Regen, 2008. **16**(1): p. 45-51.
82. Stephens, P., M. Caley, and M. Peake, *Alternatives for animal wound model systems.* Methods Mol Biol, 2013. **1037**: p. 177-201.
83. Paul Ehrlich, H., et al., *Elucidating the mechanism of wound contraction: rapid versus sustained myosin ATPase activity in attached-delayed-released compared with free-floating fibroblast-populated collagen lattices.* Wound Repair Regen, 2006. **14**(5): p. 625-32.
84. Mukhopadhyay, A., et al., *Conditioned medium from keloid keratinocyte/keloid fibroblast coculture induces contraction of fibroblast-populated collagen lattices.* Br J Dermatol, 2005. **152**(4): p. 639-45.
85. Bell, E., et al., *Development and use of a living skin equivalent.* Plast Reconstr Surg, 1981. **67**(3): p. 386-92.
86. Lu, H. and O. Rollman, *Fluorescence imaging of reepithelialization from skin explant cultures on acellular dermis.* Wound Repair Regen, 2004. **12**(5): p. 575-86.
87. Glaser, R., et al., *Stress-related changes in proinflammatory cytokine production in wounds.* Arch Gen Psychiatry, 1999. **56**(5): p. 450-6.
88. Gottrup, F., M.S. Agren, and T. Karlsmark, *Models for use in wound healing research: a survey focusing on in vitro and in vivo adult soft tissue.* Wound Repair Regen, 2000. **8**(2): p. 83-96.
89. Dyson, M., et al., *Wound healing assessment using 20 MHz ultrasound and photography.* Skin Res Technol, 2003. **9**(2): p. 116-21.

90. Kiecolt-Glaser, J.K., et al., *Slowing of wound healing by psychological stress*. *Lancet*, 1995. **346**(8984): p. 1194-6.
91. Marucha, P.T., J.K. Kiecolt-Glaser, and M. Favagehi, *Mucosal wound healing is impaired by examination stress*. *Psychosom Med*, 1998. **60**(3): p. 362-5.
92. Flanagan, M., *Improving accuracy of wound measurement in clinical practice*. *Ostomy Wound Manage*, 2003. **49**(10): p. 28-40.
93. Kuhn, C. and F. Angehrn, *Use of high-resolution ultrasound to monitor the healing of leg ulcers: a prospective single-center study*. *Skin Res Technol*, 2009. **15**(2): p. 161-7.
94. Rossi, M., et al., *The investigation of skin blood flowmotion: a new approach to study the microcirculatory impairment in vascular diseases?* *Biomed Pharmacother*, 2006. **60**(8): p. 437-42.
95. Zhai, H., et al., *Tissue viability imaging: mapping skin erythema*. *Skin Res Technol*, 2009. **15**(1): p. 14-9.
96. Haghpanah, S., et al., *Reliability of electronic versus manual wound measurement techniques*. *Arch Phys Med Rehabil*, 2006. **87**(10): p. 1396-402.
97. Abdullahi, A., S. Amini-Nik, and M.G. Jeschke, *Animal models in burn research*. *Cell Mol Life Sci*, 2014. **71**(17): p. 3241-55.
98. Wong, V.W., et al., *Surgical approaches to create murine models of human wound healing*. *J Biomed Biotechnol*, 2011 (**2011**) Article ID 969618, 8 pages.
99. Sullivan, T.P., et al., *The pig as a model for human wound healing*. *Wound Repair Regen*, 2001. **9**(2): p. 66-76.
100. Dahiya, P., *Burns as a model of SIRS*. *Front Biosci (Landmark Ed)*, 2009. **14**: p. 4962-7.
101. Kratz, G., et al., *A new in vitro model for human wound healing: effect of KCM, amniotic fluid and IGFs*. *J Cell Biochem*, 1993. **17E**: p. 133.
102. Varol, A.L. and C.D. Anderson, *A minimally invasive human in vivo cutaneous wound model for the evaluation of innate skin reactivity and healing status*. *Arch Dermatol Res*, 2010. **302**(5): p. 383-93.
103. Gissselfält, K., B. Edberg, and P. Flodin, *Synthesis and properties of degradable poly(urethane urea)s to be used for ligament reconstructions*. *Biomacromolecules*, 2002. **3**(5): p. 951-8.
104. Nilsson, K., F. Buzsaky, and K. Mosbach, *Growth of anchorage-dependent cells on macroporous microcarriers*. *Nature Biotechnology*, 1986. **4**: p. 989-990.

105. Kratz, G., *Modeling of wound healing processes in human skin using tissue culture*. *Microsc Res Tech*, 1998. **42**(5): p. 345-50.
106. O'Doherty, J., et al., *Sub-epidermal imaging using polarized light spectroscopy for assessment of skin microcirculation*. *Skin Res Technol*, 2007. **13**(4): p. 472-84.
107. McNamara, P.M., et al., *Tissue viability (TiVi) imaging: temporal effects of local occlusion studies in the volar forearm*. *J Biophotonics*, 2010. **3**(1-2): p. 66-74.
108. Görg, A., et al., *2-DE with IPGs*. *Electrophoresis*, 2009. **30 Suppl 1**: p. S122-32.
109. Shevchenko, A., et al., *Mass spectrometric sequencing of proteins silver-stained polyacrylamide gels*. *Anal Chem*, 1996. **68**(5): p. 850-8.
110. Ghafouri, B., et al., *Newly identified proteins in human nasal lavage fluid from non-smokers and smokers using two-dimensional gel electrophoresis and peptide mass fingerprinting*. *Proteomics*, 2002. **2**(1): p. 112-20.
111. Wold, S., M. Sjöström, and A. Eriksson, *PLS-regression: a basic tool of chemometrics*. *Chemometr. Intell. Lab. ,* 2001. **58**: p. 109-30.
112. Liljensten, E., et al., *Studies of polyurethane urea bands for ACL reconstruction*. *J Mater Sci Mater Med*, 2002. **13**(4): p. 351-9.
113. Nilsson, A., et al., *Results from a degradable TMC joint Spacer (Artelon) compared with tendon arthroplasty*. *J Hand Surg Am*, 2005. **30**(2): p. 380-9.
114. Gustafson, C.J., et al., *Employing human keratinocytes cultured on macroporous gelatin spheres to treat full thickness-wounds: an in vivo study on athymic rats*. *Burns*, 2007. **33**(6): p. 726-35.
115. Huss, F.R., et al., *Macroporous gelatine spheres as culture substrate, transplantation vehicle, and biodegradable scaffold for guided regeneration of soft tissues. In vivo study in nude mice*. *J Plast Reconstr Aesthet Surg*, 2007. **60**(5): p. 543-55.
116. Kratz, G., B. Palmer, and A. Haegerstrand, *Effects of keratinocyte conditioned medium, amniotic fluid and EGF in reepithelialization of human skin wounds in vitro*. *Eur J Plast Surg*, 1995. **18**: p. 209-13.
117. Longaker, M.T., et al., *Studies in fetal wound healing. IV. Hyaluronic acid-stimulating activity distinguishes fetal wound fluid from adult wound fluid*. *Ann Surg*, 1989. **210**(5): p. 667-72.
118. Tammi, R., et al., *Degradation of newly synthesized high molecular mass hyaluronan in the epidermal and dermal compartments of human skin in organ culture*. *J Invest Dermatol*, 1991. **97**(1): p. 126-30.

119. David-Raoudi, M., et al., *Differential effects of hyaluronan and its fragments on fibroblasts: relation to wound healing*. Wound Repair Regen, 2008. **16**(2): p. 274-87.
120. Jiang, D., J. Liang, and P.W. Noble, *Hyaluronan as an immune regulator in human diseases*. Physiol Rev, 2011. **91**(1): p. 221-64.
121. Birch, H.E. and G. Schreiber, *Transcriptional regulation of plasma protein synthesis during inflammation*. J Biol Chem, 1986. **261**(18): p. 8077-80.
122. Lawrence, S.O. and P.J. Simpson-Haidaris, *Regulated de novo biosynthesis of fibrinogen in extrahepatic epithelial cells in response to inflammation*. Thromb Haemost, 2004. **92**(2): p. 234-43.
123. Heizmann, C.W., G. Fritz, and B.W. Schafer, *S100 proteins: structure, functions and pathology*. Front Biosci, 2002. **7**: p. d1356-68.
124. Zimmer, D.B., et al., *The S100 protein family: history, function, and expression*. Brain Res Bull, 1995. **37**(4): p. 417-29.
125. Li, J., et al., *S100A expression in normal corneal-limbal epithelial cells and ocular surface squamous cell carcinoma tissue*. Mol Vis, 2011. **17**: p. 2263-71.
126. Li, C., F. Zhang, and Y. Wang, *S100A proteins in the pathogenesis of experimental corneal neovascularization*. Mol Vis, 2010. **16**: p. 2225-35.
127. Hines, K.M., et al., *Biomolecular signatures of diabetic wound healing by structural mass spectrometry*. Anal Chem, 2013. **85**(7): p. 3651-9.
128. Hessian, P.A., J. Edgeworth, and N. Hogg, *MRP-8 and MRP-14, two abundant Ca(2+)-binding proteins of neutrophils and monocytes*. J Leukoc Biol, 1993. **53**(2): p. 197-204.
129. Wu, N. and J.M. Davidson, *Migration inhibitory factor-related protein (MRP)8 and MRP14 are differentially expressed in free-electron laser and scalpel incisions*. Wound Repair Regen, 2004. **12**(3): p. 327-36.

*"Tappa inte sugen, världen är full av tappade sugar."*

Farmor Ulla Svensson (1928-2011)

# Papers

The articles associated with this thesis have been removed for copyright reasons. For more details about these see:

<http://urn.kb.se/resolve?urn=urn:nbn:se:liu:diva-115598>